Histol Histopathol (2004) 19: 823-844

http://www.hh.um.es

Histology and Histopathology

Cellular and Molecular Biology

Intra- and extracellular Aß and PHF in clinically evaluated cases of Alzheimer's disease

P. Fernández-Vizarra, A.P. Fernández, S. Castro-Blanco, J. Serrano, M.L. Bentura, R. Martínez-Murillo, A. Martinez and J. Rodrigo

Department of Neuroanatomy and Cell Biology, Instituto Cajal (CSIC), Madrid, Spain

Summary. Temporal cortical sections from postmortem brains of individuals without any dementing condition and with different degrees of severity of Alzheimer's disease (AD) evaluated by the Clinical Dementia Rating scale (CDR 0-CDR 3) were analyzed using immunohistochemical procedures. To demonstrate the amyloid-ß-peptide (Aß) deposition and the neurofibrillary pathology, two monoclonal antibodies were used, a human CERAD Aß (10D5) antibody raised against the N-terminal region of the Aß-peptide, and an antibody raised against paired helical filaments (PHF-1). The neuron cell bodies and the glial cells were also recognized by two polyclonal antibodies raised, respectively, against the protein gene peptide (PGP 9.5) and glial fibrillary acidic protein (GFAP). Directly related to severity of AD, progressive deposits of Aß-peptide were found within cortical pyramidal-like neurons and forming senile plaques. Ultrastructurally, Aß-peptide deposits were related to neuronal intracytoplasmic organelles, such as the ER, the mitochondria, the Nissl bodies and lipofuscin. We have also found that the intracellular deposition of the Aß peptide is a neuropathological finding prior to the appearance of PHF-immunoreactive structures. We suggest that the intracellular Aß deposition in cortical pyramidal neurons is a first neurodegenerative event in AD development and that it is involved in cell dysfunction, neuronal death, and plaque formation.

Key words: Immunohistochemistry, Alzheimer's disease, Intracellular Aß, Senile plaque formation, Human brain

Offprint requests to: Dr. J. Rodrigo, Department of Neuroanatomy and Cell Biology, Instituto Cajal (CSIC), Avenida del Doctor Arce 37, E-28002 Madrid, Spain. Fax: 34-91-5854754. e-mail: rodmart@cajal.csic.es

Introduction

Alzheimer's disease (AD) is the most common progressive neurodegenerative disorder. This disease affects individuals of all races and ethnic groups, causing up to 90% of dementia in advanced age, and it is the major health, scientific and socio-economical problem in different communities. The early diagnostic, aetiological, and molecular mechanisms of this disorder are still unclear due to lack of specific biomarkers, despite considerable progress in genetic, clinical, and basic neuroscience.

This syndrome is characterized by a progressive neurodegeneration, memory loss, and intellectual and emotional dysfunctions (Selkoe, 1994; Terry, 1994; Jellinger and Bancher, 1998; Malchiodi-Albedi et al., 2001), as well as by changes in neuroendocrine and autonomic functions (Raskind et al., 1982; Spar and Gerner, 1982; Balldin et al., 1983; Iacono and Sandyck, 1987; Christie et al., 1987). The histopathological findings include deposition of amyloid-ß-peptides (Aß) of 40-42 amino-acid (Gandy and Greengard, 1992; Jellinger, 1998) to form senile plaques (SP) and amyloid angiopathy, cytoskeletal changes, such as neurofibrillary tangles (NFT), distrophic neurites forming neuritic plaques, and neuropil threads, containing polymerised hyperphosphorylated tau protein triplet, or masses of paired, helical filaments (PHF) (Kondo et al., 1988; Wischik et al., 1988; Bondareff et al., 1990; Caputo et al., 1992; Novak et al., 1993), cerebral atrophy, and astrogliosis. These findings indicate the main origin of the loss of neurons and synapses, as well as cortico-cortical disconnection of the cerebral cortex (DeKosky and Scheff, 1990; Selkoe, 1994; Terry, 1994; Jellinger and Bancher, 1998; Malchiodi-Albedi et al., 2001). Some of these neuropathological structures were also found in the brain of non-demented elderly people (Rothchild, 1937; Tomlinson et al., 1968; Terry and Katzman, 1983; Crystal et al., 1988; Katzman et al., 1988; Mann and Esiri, 1989; Delaere et al., 1990; Dickson et al., 1991). The NFT and SP are present in virtually all cases of AD, but are not uniformly

distributed throughout the forebrain (Hirano and Zimmerman, 1962; Ishii, 1966; Ball, 1977, 1978; Hyman et al., 1984, 1988; Ulrich and Stahelin, 1984; Ulrich et al., 1987; Saper and German, 1987; German et al., 1987; Terry et al., 1987; Berg, 1988; Braak and Braak, 1991, 1992; Byne et al., 1991; Price et al., 1991; Arriagada et al., 1992; Braak et al., 1994; Good et al., 1996; Nagy et al., 1997; Arendt et al., 1998).

It is generally accepted that the number of these neuropathological findings correlate with the degree of cognitive impairment (Blessed et al., 1968), but factors such as the loss of synapses or presynaptic marker proteins (Masliah et al., 1989; DeKosky and Scheff, 1990; Terry et al., 1991) or neuritic change (McKee et al., 1991) may correlate better with functional impairment.

It is also accepted that certain mechanisms mediating neuronal plasticity, proliferation and differentiation participate in AD (Arendt et al., 1986, 1997, 1998; Heintz, 1993; Arendt, 1993, 2000). The vascular factor is also increasingly involved in the pathogenesis of AD (Grammas, 2000).

During the last years it has become evident that the Aß component of SP, derived from a larger precursor protein known as the amyloid precursor protein (APP), may be the key molecule in the pathology of AD, but its source and its neurotoxic actions are, however, still a matter of controversy. Historically, the origin of SP has been assumed to be extracellular. Nevertheless, recently particular interest has been shown in the theoretical model for the generation of SP (Wilson et al., 1999). That is, Aß42 is generated in the neuronal endoplasmic reticulum (ER) under normal circumstances and increased in patients of familiar AD (FAD). All these events were recently summarized (Gyure et al., 2001) in the following sequence: i) intracellular accumulation of Aß in neurons and astrocytes, ii) deposition of extracellular Aß and formation of diffuse plaques, and iii) development of neuritic plaques and NFT with activation of microglia.

The aim of the present work was to establish the intimate correlation between the neuropathological hallmarks of AD and its progressive clinical severity, in postmortem brains of individuals without any dementing condition and with different degrees of severity of AD evaluated by the Clinical Dementia Rating scale. Immunohistochemical procedures were applied to demonstrate the progressive intra- and extracellular deposition of Aß peptide and neurofibrillary changes in temporal sections.

Materials and methods

Selection and collection of material

The brains were obtained postmortem from individuals who had been clinically studied in the Memory and Aging Project (MAP) of the Washington University Alzheimer's Disease Research Center (ADCR) and generously supplied by Dr. J. Price (Washington University School of Medicine). The assessment protocol provided sufficient information for the clinician to determine the presence or absence of dementia and to rate the severity of the dementia present, according to the Clinical Dementia Rating (CDR) scale (Berg, 1988; Burke et al., 1988; Morris et al., 1988, 1991; Price et al., 1991; Price and Morris, 1999). The CDR scale, previously standardized neuropathologically (Berg, 1988; Burke et al., 1988; Morris et al., 1988; Price et al., 1991), is directly linked to validated clinical diagnostic criteria for senile dementia of AD type (SDAT) (Morris et al., 1988; Morris, 1997). The clinical protocol included interviews of the patients and informants to compile the information necessary to rate the subjects' cognitive performance in six domains: memory, orientation, judgement and problem solving, community affairs, home and hobbies, and personal care. The CDR has been standardized for multicenter use and has also been validated neuropathologically, particularly in the presence or absence of dementia. Procedures for the MAP included criteria that ensure that the SDAT was the only mental disorder found to be present (Berg et al., 1982; Morris, 1993; Morris, 1997).

In samples selected to be free of other potentially dementing conditions, a CDR score of 0.5 or greater is associated with histological and clinical diagnosis of AD, whereas a CDR score of 0 is associated with few or no AD neuropathological lesions (Morris et al., 1991, 1996; Berg et al., 1993; Morris, 1997).

This present study was performed on temporal sections of individuals with neither dementia nor the histopathological markers of AD (CDR 0, ages 53, 60, 92 years old), without dementia but with the histopathological markers of AD (CDR 0 preclinical, ages 74, 76, 79, 88, 93 years old) (Price and Morris, 1999), with very mild cognitive dysfunction (CDR 0.5, ages 78, 80, 89, 91 years old), as well as with mild (CDR 1, ages 89, 95, 97 years old), moderate (CDR 2, ages 69, 75, 76 years old) and severe dementia (CDR 3, ages 79, 82, 85, 87 years old).

Antibodies

To demonstrate the specific immunoreactive lesions of AD on temporal cortical sections, we used polyclonal and monoclonal antibodies. Aß immunoreactivity was visualized using a specific monoclonal antibody raised against a synthetic peptide containing residues 1-38 of human Aß (CERAD 10D5) (Athena Neuroscience, South San Francisco, California, USA) (Hyman et al., 1992). The sequential epitope of this antibody is located at positions 3-6 within Aß and corresponds to the amino-acid sequence EFRH (Frenkel et al., 1998). 10D5 recognizes all Aß species (Liao et al., 1998; Gomez-Isla et al., 1999; Augustinack et al., 2002). The specificity of Aß 10D5 immunoreactivity was confirmed by preabsorption with Aß 1-40 (Neosystem, Strasbourg, France) and by preabsorption with a synthetic peptide

corresponding to residues 657-676 of APP (Bachem, Bubendorf, Switzerland). Preabsorption with Aß 1-40 resulted in loss of immunoreactivity in senile plaques and neurons. Similar results were obtained when the primary antibody was omitted (Fig. 1). The immunoreactivity obtained with 10D5 preabsorbed with APP657-676 was identical to that observed when using the antibody without preabsorption. This antibody has been widely used in previous histological and biochemical studies (Hyman et al., 1992; Walker et al., 1994; Frenkel et al., 1998, 1999; Gomez-Isla et al., 1999; Urbanc et al., 1999; Tucker et al., 2000; Parvizi et al, 2000, 2001 Backsai et al., 2001, 2002; Augustinack et al., 2002; Schenk, 2002).

A monoclonal antibody that detects paired helical filaments (PHF-1) (generously supplied by Dr. P Davies, Albert Einstein College of Medicine, New York) was employed to demonstrate neurofibrillary tangles, distrophic neurites, and neuropil threads. The PHF-1 epitope contains both phosphorylated Ser396 (Lang et al., 1992) and Ser404 (Otvos et al., 1994) and recognizes tau peptides containing either individually phosphorylated Ser396 or Ser404, but there is an increase in the sensitivity of detection of tau peptides by PHF-1 when both serines are phosphorylated (Otvos et al., 1994). This antibody was also used in previous immunohistochemical and biochemical studies (Greenberg et al., 1992; Hasegawa et al., 1996; Hoffman et al., 1997).

The neuron cell bodies were recognized by a polyclonal antibody marker of the protein gene peptide (PGP 9.5, supplied by Prof. JM Polak, Hammersmith Hospital, London, UK) and a polyclonal, as well as a monoclonal antibody were used to demonstrate the presence of glial fibrillary acidic protein (GFAP, Sigma CO, St. Louis MO, USA) in glial cells.

Tissue preparation

The blocks were taken from the temporal lobe (to the caudal limit of the hippocampus), fixed by immersion in buffered 10% formalin within 36 h after death. For electron-microscopy analysis, tissues were taken from postmortem brains of AD (CDR 3) and fixed by immersion in 2% paraformaldehyde and 0.1% glutaraldehyde in 0.1 M of phosphate buffer (PB). Blocks for optical studies were immersed in a cryoprotective solution (10% glycerine) for 2-4 days, and for electron-microscopy studies in 30% sucrose for 24 h. Blocks were sectioned at 50 μm on a freezing microtome or vibratome, respectively.

Immunohistochemistry

Light microscopy

In the immunohistochemical study, the ABC procedure was used to demonstrate the immunoreactive sites (Guesdon et al., 1981; Hsu and Raine, 1981; Rodrigo et al., 1994; Uttenthal et al., 1998). Free-floating sections were washed in phosphate-buffer saline (PBS) for 5 min and incubated in PBS containing 3% hydrogen peroxide for 30 min to quench the endogenous peroxidase. The sections used for Aß immuno-histochemistry were previously washed in 90% formic acid for 5 min at room temperature (Davies et al., 1988). For the prevention of non-specific staining, the sections were then preincubated for 1 h in PBS containing 0.2 % Triton X-100 and 3% normal serum from species of the secondary antibodies. Immediately afterwards, the sections were separately incubated in the primary antibodies against Aß (10D5) and PHF (PHF-1), which were diluted 1:2000 and 1:250 in 0.2 % Triton X-100, for 48 h at 4 ºC. After several washes in PBS, the sections were incubated with biotinylated secondary antibody (anti-mouse immunoglobulin, Vector Laboratories, Burlingame, CA, USA) for 1 h at room temperature. After being washed, the sections were finally incubated with peroxidase-linked ABC (Vector Laboratories, Burlingame, CA, USA) for 90 min. Peroxidase activity was demonstrated by nickel enhancement 3,3'-diaminobenzidine tetrahydrochloride (Rodrigo et al., 1994).

Electron microscopy

Fixed and cryoprotected sections were rapidly frozen in nitrogen and thawed in cold 0.1 M PB to improve antibody penetration. The immunostaining was performed as for light microscopy except that Triton X-100 was not included in the incubation solutions. The Aß-10D5 as primary antibody, diluted 1:2000 in PBS, was used to recognize the deposition of Aß. The immunohistochemical reaction was developed by incubating the tissue sections in PBS containing 0.006% 3,3'-diaminobenzidine tetrahydrochloride (DAB, Sigma. St Louis. MO) for 10 min followed by 0.003% H_2O_2 in the same solution. The DAB reaction was interrupted at different times for inspection of sections. Subsequently, the sections were washed for about 10 min in PBS and then for 10 min in PB, postfixed in 1% osmium tetroxide in 0.1 M PB (1 h), dehydrated in ethanol of increasing concentrations and block-stained in uranyl acetate (1% in 70% ethanol) in the dark, for 40 min at room temperature. The sections were mounted on Durcupan ACM resin slides (Fluka) under plastic coverslips and incubated for 3 days at 56 °C. Selected areas of the temporal cortex were dissected out, re-embedded in Durcupan and ultrathin sections were mounted on formwar-coated grids, stained with lead citrate and examined in a Jeol 1200 EX electron microscope.

Double immunostaining

Double staining was performed on sections from subjects classified on the CDR 3 scale. Double staining to PGP 9.5/Aß, PGP 9.5/PHF and GFAP/Aß was performed by incubating with primary polyclonal

antibodies (PGP 9.5 and GFAP) diluted 1:800 and 1:400, respectively, and monoclonal antibodies (Ab and PHF) diluted in PBS Triton X-100 as described above for 24 h at 4 ºC. After being washed in PBS, the sections were incubated for 2 h with secondary antibody, goat IgG anti-rabbit fluorolink Cy2-labelled (green fluorescence) to demonstrate PGP 9.5 and GFAP immunoreactive structures, and a rabbit IgG anti-mouse Cy5-labelled (red fluorescence) to demonstrate Aß and PHF (Amersham Iberica, Life Science) immunoreactive-site products. Sections were mounted in PBS/glycerol (1:9) and analyzed by a TCS laser scanning confocal image system equipped with a krypton-argon ion laser (Leica, Spain).

Immunohistochemical control

Control procedures to optical, confocal and ultrastructural studies were carried out on some sections. No immunolabeling was observed when the primary antibodies were omitted or replaced with an equivalent concentration of preimmune or normal serum from species of the secondary antibodies.

Quantification of Aß and PHF

A quantitative study was carried out for both Aß and PHF antibodies on columnar areas of 27 mm^2 of the temporal cortex. The quantitative data obtained were analyzed using one-way ANOVA and afterwards the Dunnet test to compare each experimental group with the control group. P values lesser than 0.05 were considered statistically significant.

From each individual the immunoreactive cortical images were captured using a Axioplan 2 imaging microscopy, 40x Neofluar lens (Zeiss Germany) and a SONY CCD-IRIS video-camera. The image was projected onto a grid of 3 mm^2 on a television screen (SONY Trinitron). The total cortical area analyzed for each individual (n=3) was 9 mm^2 that corresponded to 72 cortical columns.

Results

The immunohistochemical analysis to demonstrate the expression of Aß (10D5), PHF (PHF-1), PGP 9.5, and GFAP, was performed on sections of temporal cortex from postmortem brains from non-demented individuals and from AD patients with diminished or no ability to conduct everyday activities, according to the CDR scale. The CDR has been documented as a reliable and sensitive method of distinguishing non-demented aging from early dementia of AD, and to track the progression of clinically meaningful dementia by clinical trials and other clinical and anatomopathological studies (Price et al., 1991). This scale was standardized for multicenter use, including the Consortium to Establish a Registry to Alzheimer's Disease (CERAD) and Alzheimer's disease cooperative study (Morris, 1997).

Light microscopy

CDR 0

Aß expression. Intracellular Aß deposition was found in occasional neurons with pyramidal morphology of large and small size. These immunoreactive neurons were found in the cerebral temporal cortex of all individuals of this group and mainly in layers III and V (Fig. 2A). The reaction product was expressed as a granular structure and distributed in the cytoplasm of these neurons, surrounding the nuclear area (Fig. 2B,C). The granules of different size were interconnected forming a cytoplasmic reticular structure that bore a strong resemblance to the ER. Occasional SP were found in the temporal cortex in only one individual of 53 years old.

PHF expression. Occasionally, PHF-immunoreactive neurons with pyramidal or multipolar morphology were found in this CDR 0 scale, mainly distributed in layer III, but some neurons were also found in layers V and VI of the temporal cortex (Fig. 2D). The number of PHF neurons was less than that of Aß immunoreactive neurons in this CDR scale.

The reaction product showed a more or less granular appearance and was homogeneously distributed in the neuronal cytoplasm (Fig. 2E, F) and the proximal portion of their processes. Some filamentous structures were also found in the cytoplasm of PHF-containing neurons, contributing to the formation of incipient NFT. Irregularly stained processes, surrounded by scattered fragmented fibrils with a curved or straight course, contributed to the formation of incipient or occasional immunoreactive cortical neuropil threads.

CDR 0 preclinical

Aß expression. Sections of the temporal cortex from postmortem brains clinically evaluated as the CDR 0 preclinical scale showed some Aß immunoreactive pyramidal-like neurons and SP. The number of both immunoreactive structures was scarce, but increased with respect to the CDR 0 subjects (Fig. 3A).

Immunoreactive pyramidal-like, pyriform, or round neurons were found in layers IIIa, IIIb (Figs. 3B-F) and occasionally in layers II and V. The reaction product, as a granular structure, was distributed throughout the cytoplasm and in the proximal portion of some processes. The intracellular deposits of the reaction product, as a reticular structure with nodes interconnected by short, irregular immunoreactive filamentous tracts, differed in size and morphology.

The amyloid plaques were low in number, clearly differing in size, distribution, and morphology. Some SP were large or medium-sized and distributed in the upper layers II, IIIa, and IIIb. Small SP were occasionally found in layers IV and V.

The senile plaques displayed wide morphological variety. Some of them showed pyriform morphology and

others had a round shape with a reticular structure and irregular external borders. Some SP included non-stained round or pyriform neuronal structures (Fig. 3G). Finally, some Aß plaques showed a central mass of reaction product surrounded by a ring of reticular reactive material with an irregular external limit caused by the presence of small or punctate immunoreactive Aß deposits (Fig. 3H). Between these morphologies, sizes and locations of Aß, many transitional morphological plaques could be found.

PHF expression. Immunoreactive neurons with pyramidal morphology were found distributed in layers II and III. Normally, the number of these neurons was scarce, but sections from some individuals of this group showed a higher number of these neurons distributed in the upper cortical layers (Fig. 3I).

The sections studied in this CDR scale showed a

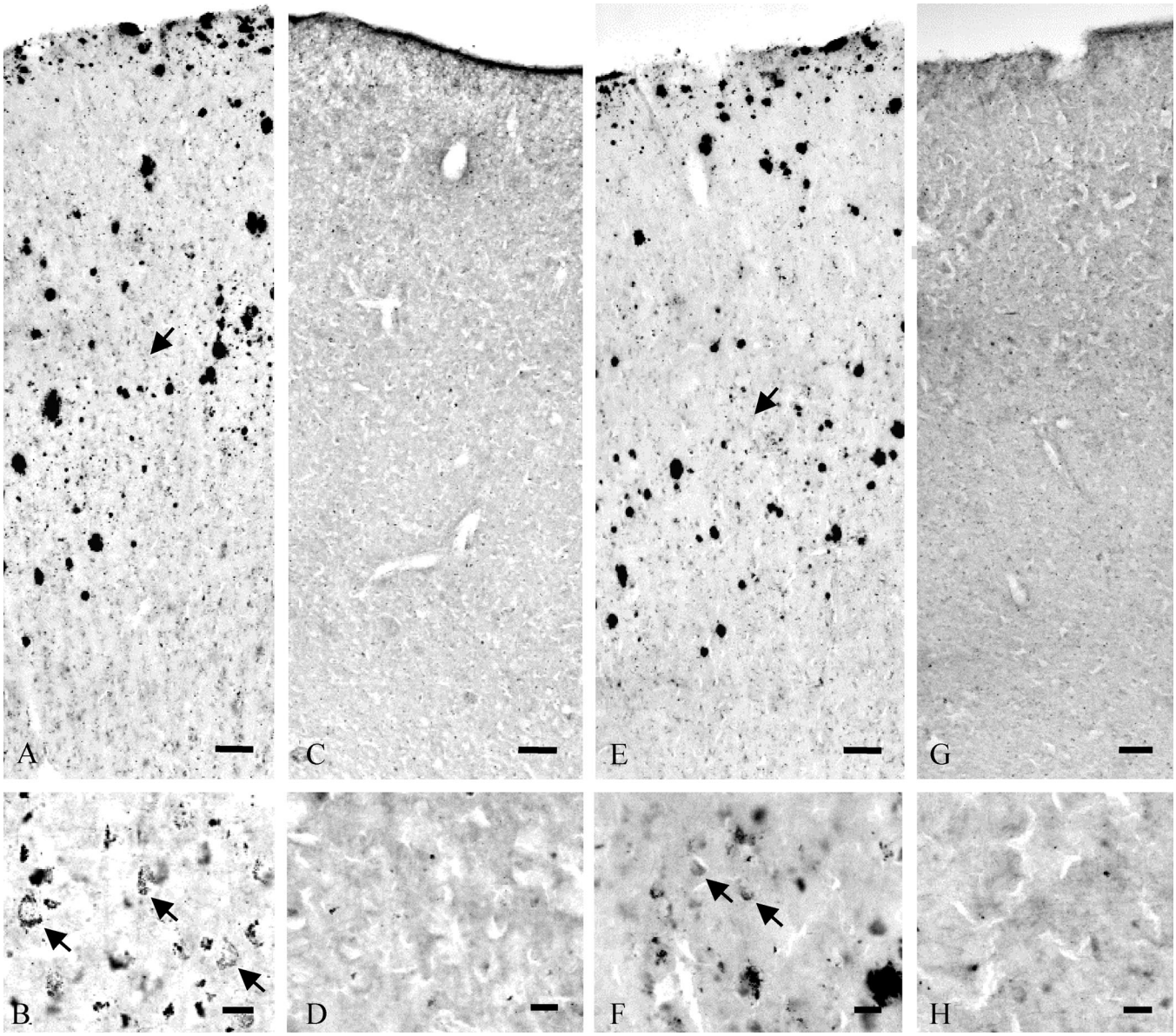

Fig. 1. The specificity of Aß 10D5 immunoreactivity is confirmed by preabsorption with Aß 1-40 and $APP_{657-676}$ and by omission of the primary antibody. Consecutive sections of cerebral temporal cortex from the same individual are stained with the Aß antibody without preabsorption **(A and B)**, preabsorbed with Aß1-40 **(C and D)**, and preabsorbed with $APP_{657-676}$ **(E and F)**, and the primary antibody is omitted in **(G and H)**. Senile plaques and pyramidal neurons (arrows) are observed when the section is stained with Aß (10D5) without preabsorption **(A and B)** and when the Aß antibody is preabsorbed with $APP_{657-676}$ **(E and F).** Preabsorption with Aß 1-40 **(C and D)** and omission of the primary antibody **(G and H)** results in loss of immunoreactivity both in senile plaques and in neurons. Scale bars: A,C,E and G, 100 μm; B, D, F and H, 20 μm.

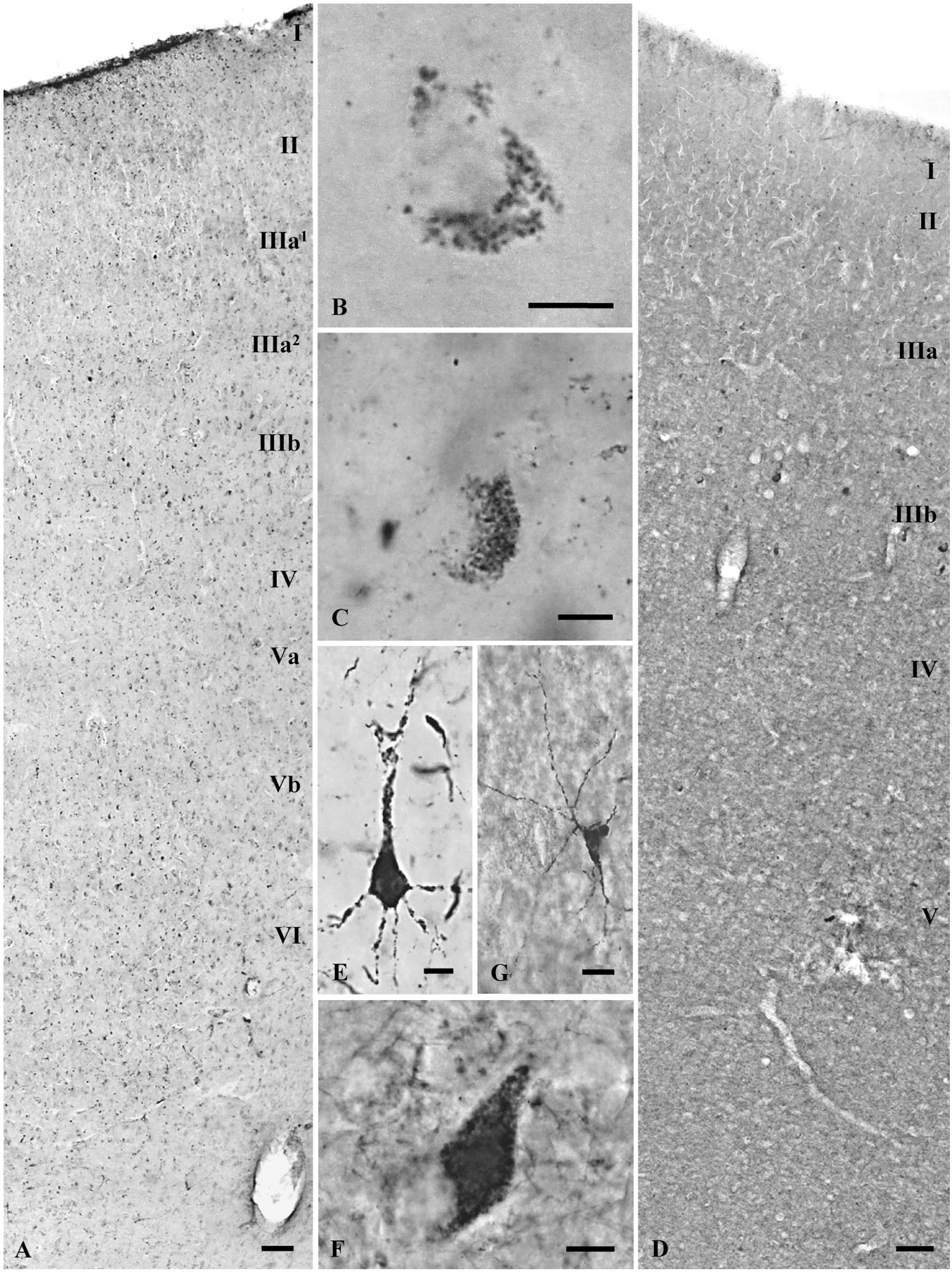

Fig. 2. Aß **(A)** and PHF **(D)** expression in the temporal cortex from postmortem brains of AD patients, CDR 0. **(B and C)** show the Aß reaction product distributed in the cytoplasm of occasional pyramidal-like neurons in layer IIIb. PHF neurons with multipolar **(G**) and pyramidal **(E, F)** morphology in layers V and IIIb, respectively. Scale bars: A, D, 100 μm; B, C, F, 10, μm; E, G, 20 μm.

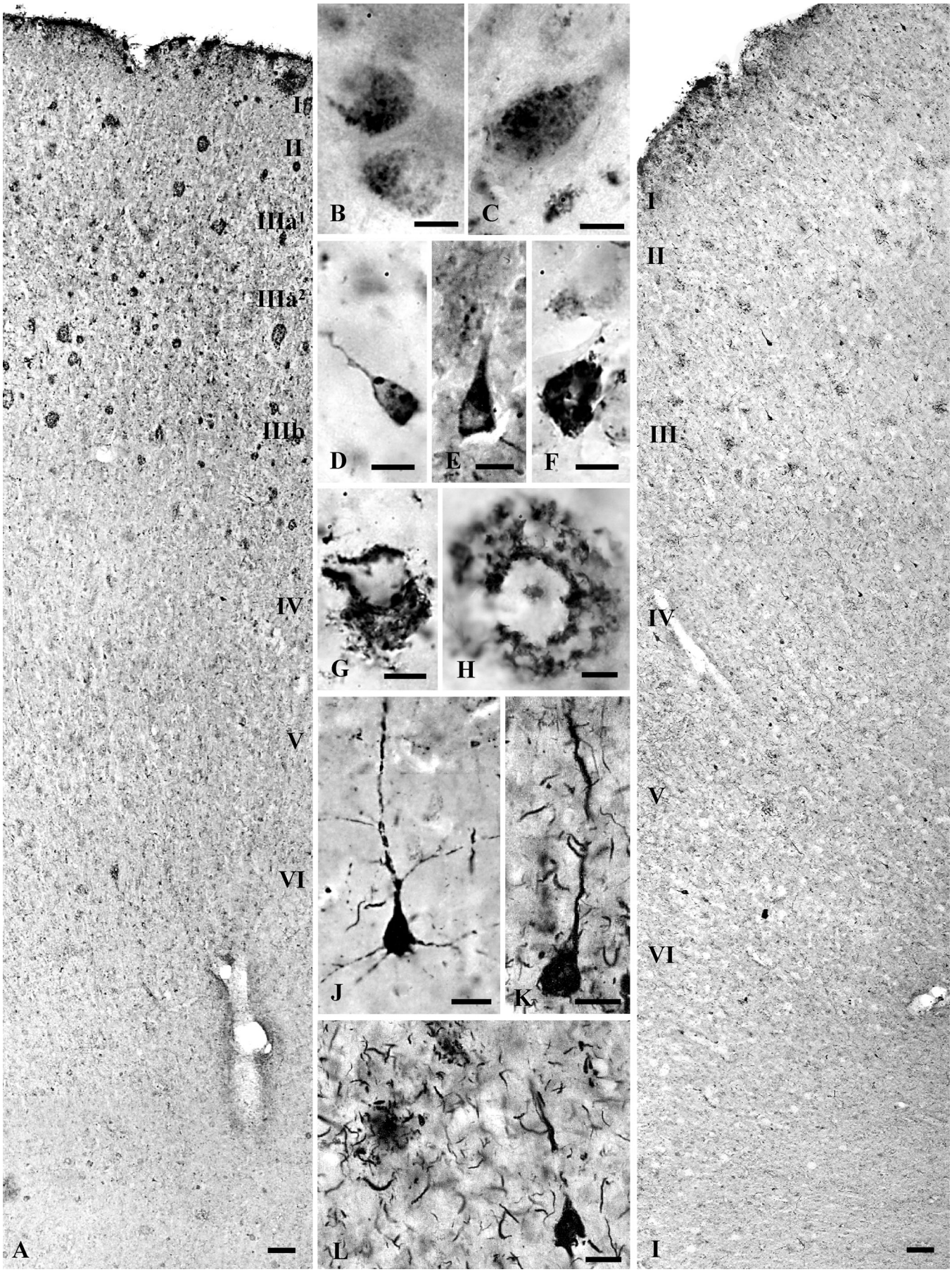

Fig. 3. Aß **(A)** and PHF **(I)** expression and distribution in the temporal cortex from postmortem brains of AD patients, CDR 0 preclinical. **B-F.** Pyramidal-like immunoreactive neurons in layer III containing the Aß reaction product with granular morphology. **G and H.** Two morphological types of senile plaques. **J and K.** PHF-immunoreactive neurons and swollen fragments of dystrophic cortical neurites in layer III. **L.** corresponds to neuritic plaques and neuropil threads in layer III. Scale bars: A, I, 100 μm; B, C, 10 μm; D-H, J-L, 20 μm.

scarce number of neurons containing PHF-immunoreactive filamentous structures as incipient NFT. These filamentous structures were found in the cytoplasm and in the short or fragmented processes that pervaded the next parenchyma (Fig. 3J-L). The reaction product, as granular or filamentous morphological complexes, was divided into plots or homogeneously distributed through the neuronal cytoplasmic cell body and the basal or apical processes of these pyramidal-like neurons.

Sometimes, swollen stained fragments of dystrophic cortical neurites with a tortuous, curved course and a blurred outline contributed to the formation of the neuritic plaques or the neuropil threads (Fig. 3L).

CDR 0.5

Aß expression. Usually, the two main Aß immunoreactive structures, neurons and SP, were increased in number in relation to the previous CDR scale and mainly distributed in III, V and VI cortical layers (Fig. 4A). Some neurons showed a pyramidal morphology containing Aß deposits distributed through the cytoplasm and in the proximal portion of their dendritic processes. The reaction product was found with a reticular or irregular filamentous morphology. Some of the Aß-immunoreactive structures were found to have a striking appearance. These displayed a pyramidal morphology with the perikaryon strongly swollen without a clear structure with an irregular outline and more or less homogeneously stained (Fig. 4B,D).

The SP differed in size and morphology. Large SP were found with a reticular and irregular structure and were distributed in all cortical layers (Fig. 4F,G). Some large SP, looking like a wheel, showed reactive material distributed in one external ring that surrounded an internal, central or nuclear accumulation of reactive material (Fig. 4F). Both reactive areas were interconnected by radial tracts of immunoreactive product. Sometimes, the SP contained non-reactive structures such as small neuronal cell bodies (Fig. 4G). Finally, some large or medium-sized SP were surrounded by numerous accumulations of amyloid material, originating from the periphery of the large SP and forming an extensive constellation.

PHF expression. PHF-immunoreactive structures were increased in relation to the previous CDR scale and distributed through the cortical layers III and V and occasionally VI (Fig. 4H). Some scattered immunoreactive neurons with a pyramidal morphology were found containing NFT. Swollen and fragmented dystrophic neurites with a straight, curved or tortuous course, forming neuritic plaques or neuropil threads (Fig. 4I-L) were also increased in relation to the previous CDR scales.

However, comparing the PHF immunoreactivity to the Aß immunoreactivity, the number of PHF immunoreactive structures was lower than those immunoreactive to Aß.

CDR 1

Aß expression. Aß-immunoreactive pyramidal-like or pyriform neurons were found forming three clear laminations in layers I, III and V (Fig. 5A). We also found striking Aß-containing structures that displayed a pyramidal morphology and showed the immunoreaction product as reticular or granular deposits distributed throughout the cytoplasm. In some cases, these accumulations of reaction product were found surrounding an unstained central nuclear area and in the proximal portion of the main and large processes (Fig. 5B-E). From the external cellular membrane of some immunoreactive pyramidal-like structures, small protrusions containing Aß reaction product emerged, exhibiting an irregular outline (Fig. 5E).

The SP were increased in number in this CDR scale, showing different morphology and size (Fig. 5F,G). Large compact plaques were found containing an immunoreactive core surrounded or not by a small, reticular ring of Aß material. Sometimes, the plaques were surrounded by a variable number of disaggregated small, reticular accumulations of Aß material, containing or surrounding unstained cell bodies.

PHF expression. The immunoreactive neurons and neuritic plaques were dramatically increased in relation to the previous CDR scales, but a different immunoreactive pattern was found between all individuals studied. Generally, the distribution of PHF-immunoreactive structures was found in layers II-III and V (Fig. 5H). Pyramidal-like neurons contained NFT and an immunoreactive reticular cytoplasmic structure. The proximal portion of the processes was also filamentous and swollen with a tortuous, curved, or straight course, which pervaded the next cortical layers forming the neuropil threads (Fig. 5I). Some tortuous processes were found forming neuritic plaques (Fig. 5J).

CDR 2

Aß expression. Aß immunoreactivity increased and small or large aggregates of Aß material were found in all cortical layers (Fig. 6A). Two main cellular types containing Aß were found in this CDR scale. The first type had a pyramidal morphology and was distributed in all cortical layers, but preferentially in layers III and V (Fig. 6B,C). These neurons exhibited a large cytoplasm and short processes containing granular or reticular deposits of reaction product with or without homogeneous distribution. The second type was of small size, like glial cells, and showed short, tortuous processes and numerous short collaterals distributed in the close proximity.

The SP were increased in size and number and distributed in all cortical layers. The most numerous showed an irregular outline and formed dense and fragmented accumulations of interconnected Aß reaction product, including sometimes unstained structures like

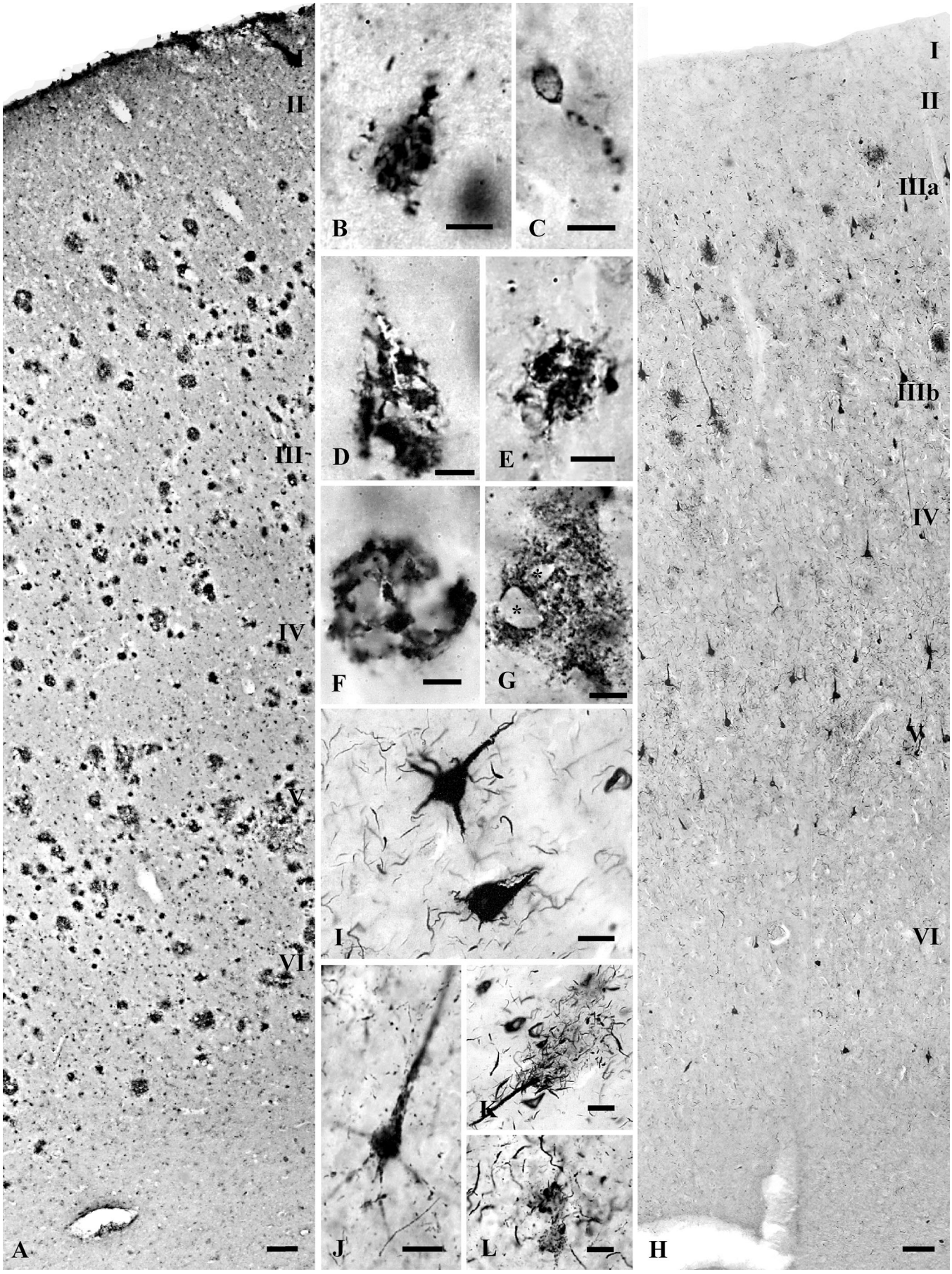

Fig. 4. Aß **(A)** and PHF **(H)** expression and distribution in the temporal cortex from postmortem brains of AD patients, CDR 0.5. **B-D.** Intracellular Aß deposits in neurons with pyramidal morphology in layer III. **E-G.** Different morphological types of senile plaques in layer III containing masses of Aß reaction product surrounding unreactive neuronal bodies (asterisks). **I-L.** show the morphology of immunoreactive neurons to PHF, layers III **(J, K)** and V **(I, L)**. **K and L** show the structure and morphology of the neuropil threads and neuritic plaques. Scale bars: A, H, 100 μm; B-G, I-L, 20 μm.

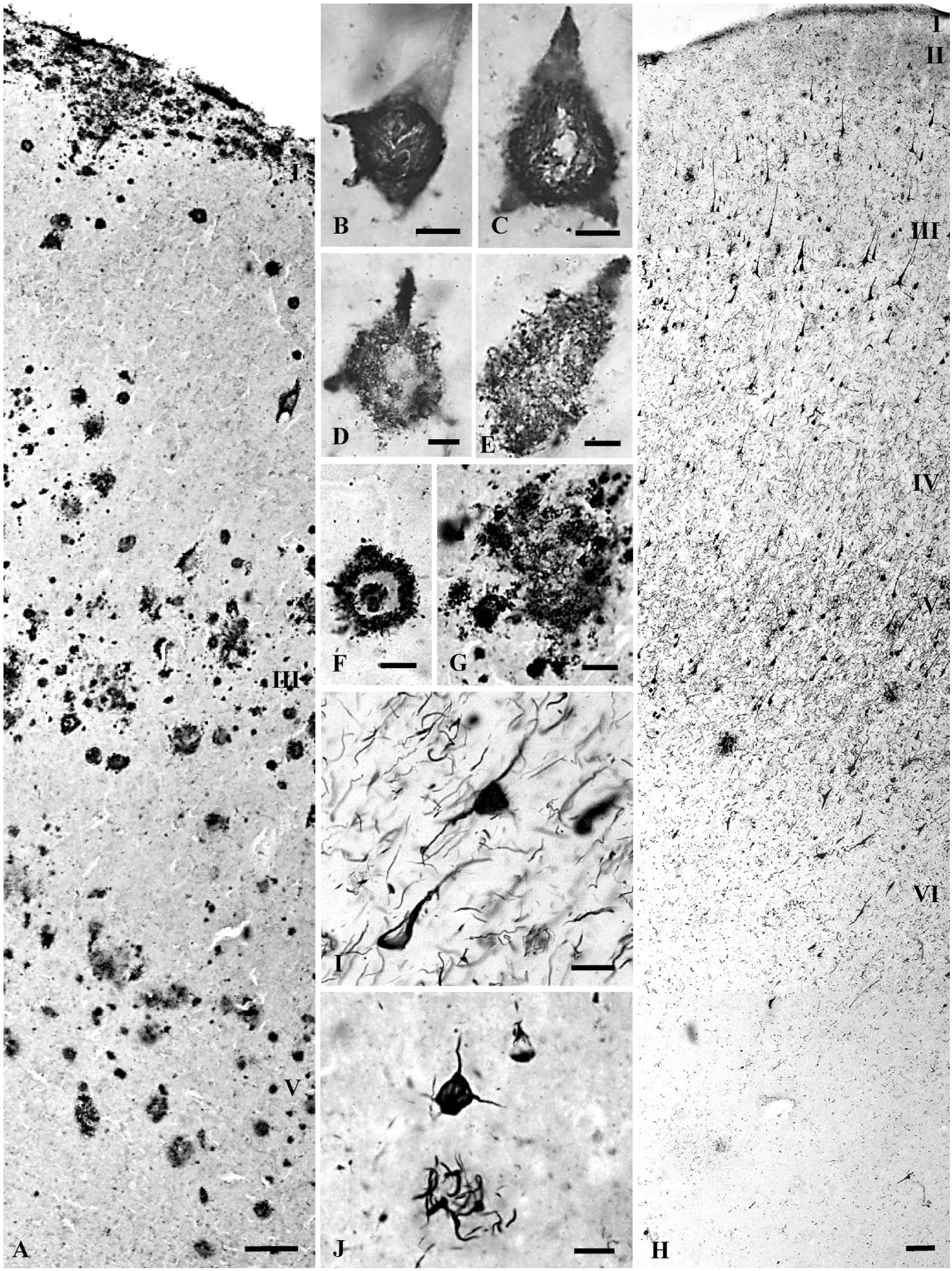

Fig. 5. Aß **(A)** and PHF **(H)** expression and distribution in the cerebral temporal cortex from postmortem brains of AD patients, CDR1. **B-E** show the granular and reticular morphology of Aß-reactive product apparently with intracellular distribution in pyramidal-like cortical neurons. **F and G** show the distribution of Aß reaction product forming senile plaques. **I and J** show the morphology of a PHF-immunoreactive cortical neuron and some dystrophic cortical neurites. Scale bars: A, H, 100 μm; B-E, 10 μm; F, G, I, J, 20 μm.

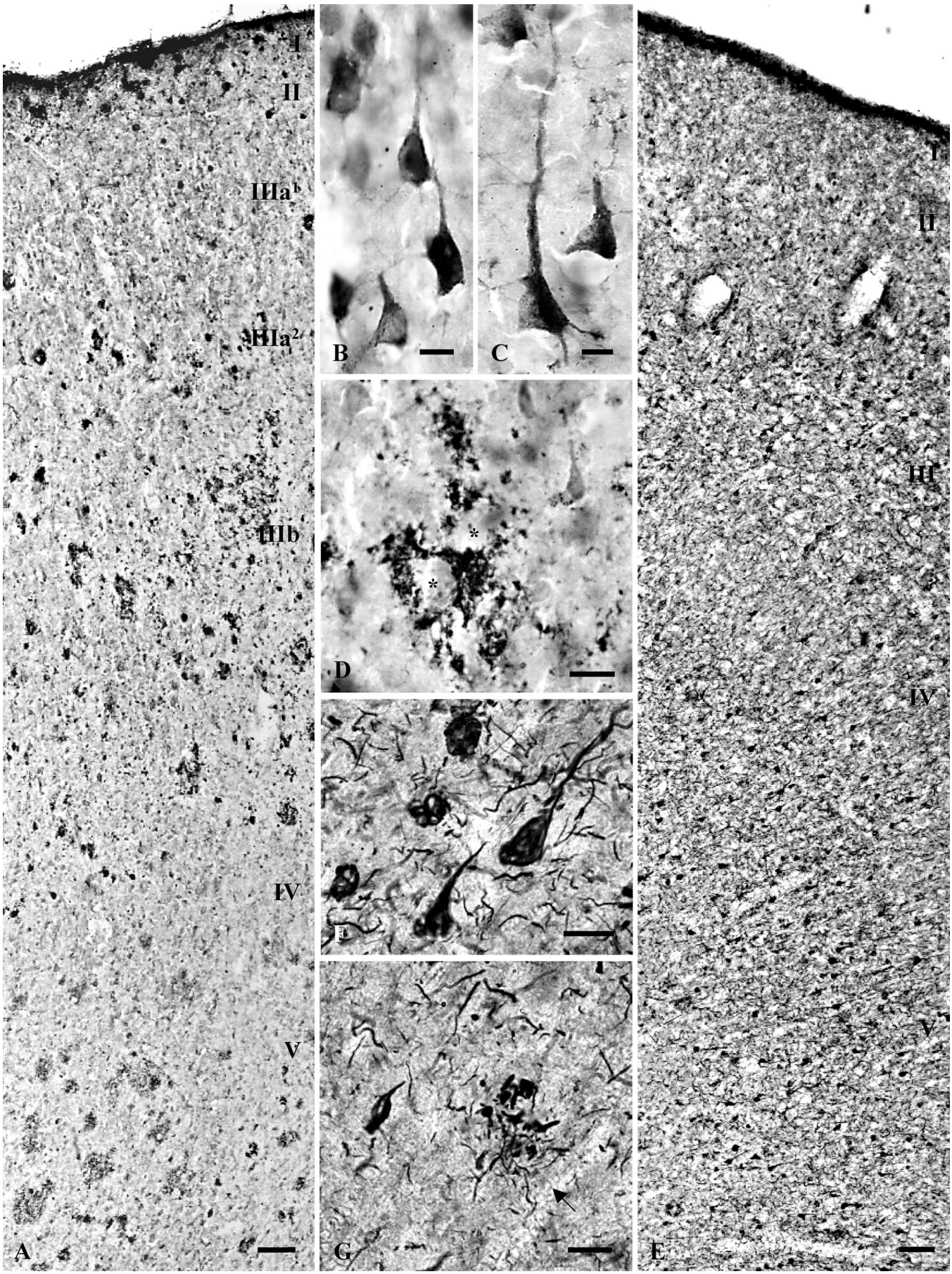

Fig. 6. Aß **(A)** and PHF **(E)** expression and distribution in the cerebral temporal cortex from postmortem brains of AD patients, CDR2. **B and C** show different types of Aß immunoreactive neurons in layers IIIa and IIIb, respectively. **D** corresponds to singular masses of Aß in layer V surrounding unreactive neurons (asterisks) forming senile plaques. **F and G** show the morphology of intracellular PHF immunoreactivity in layer V and dystrophic neurites in layer VI forming neuritic plaques (arrow), respectively. Scale bars: A, E, 100 μm; B, C, 10 μm; D, F, G, 20 μm.

neuronal cell bodies (Fig. 6D).

PHF expression. The number of PHF-immunoreactive structures was increased in this CDR scale. Virtually all cortical layers contained PHF immunoreactive structures, which corresponded to NFT, neuritic plaques, and neuropil threads (Fig. 6E). Large pyramidal-like neurons containing PHF showed a filamentous appearance of variable complexity and a cytoplasmic reticular structure (Fig. 6F). The processes of these neurons were vacuolated and fragmented, with short sinuous and tortuous short collaterals, which were surrounded by swollen short fragments of fibrils that contributed to the formation of the neuropil threads (Fig. 6G).

CDR 3

Aß expression. Aß immunoreactive structures were increased in all cortical layers of the temporal cortex (Fig. 7A). Layer I showed small immunoreactive Aß deposits and neurons of a small size surrounding the blood vessels that penetrated into the cortex from the pial blood vessels. Numerous Aß immunoreactive neurons showing a pyramidal or multipolar morphology with tortuous, varicose, fragmented, swollen, or irregular processes were found between layers III and V. These stained neurons showed an irregular somatic outline, laminar protrusions and destructurated cytoplasm because of the presence of compact and reticular deposits of reaction product (Fig. 7B,D,E). Aß-containing structures similar to those found in the CDR 0.5 scale were also found. These were either small or large and displayed a pyramidal morphology with Aß deposits, with the apearance of interconnected aggregates, looking like incipient SP (Fig. 7F,G,I). Some small structures similar to glial cells contained Aß immunoreactivity (Fig. 7C).

SP were mainly distributed in all cortical layers. Layers IIIa and IIIb showed special relevance, containing a scarce number of large SP which were surrounded by numerous small, scattered accumulations of Aß reaction product. These small accumulations were isolated or interconnected by reticular filaments forming a complex structure, which included small or medium non-reactive cells. Layer VI showed few but large SP (Fig. 7J,K).

PHF expression. PHF immunoreactivity was extensively increased in this CDR scale. All cortical layers contained numerous neurons with NFT, and immunoreactive fibrils forming the neuropil threads and neuritic plaques of different size and morphology (Fig. 7L). Neurons with pyramidal, fusiform, or multipolar morphology showed a filamentous cytoplasm forming NFT (Fig. 7M). A few numbers of neurons with granular PHF immunoreactivity were also found. The processes originated from immunoreactive neurons with a reticular morphology and an irregular border which, because of the presence of immunoreactive laminated protrusions and short fragmented collaterals, contributed to form the neuropil threads and neuritic plaques in all cortical layers (Fig. 7N).

Confocal microscopy

The coexistence between Aß/PGP 9.5, Aß/GFAP, and PHF/PGP 9.5 was analyzed by confocal microscopy.

PGP 9.5/Aß expression

PGP 9.5, as a neuronal marker, was found in numerous neurons (green colour) (Fig. 8A), many of which also contained Aß deposits (red colour) (Fig. 8B), as granular structures (Fig. 8C). A variable number of PGP 9.5-immunoreactive neurons (Fig. 8D), containing or not Aß deposits (Fig. 8E) were included or surrounded the large or medium-sized Aß deposits that formed the SP (Fig. 8F). The SP were isolated or surrounded by small fragments of Aß material penetrating into the next neural parenchyma.

PGP 9.5/PHF expression

Numerous neurons containing the neuronal marker PGP 9.5 (green colour) (Fig. 8G) showed PHF (red colour) immunoreactivity (Figs. 8H). The coexistence of PGP 9.5/PHF was also found in some neuritic plaques, and when forming the neuropil threads (Fig. 8I).

GFAP/Aß expression

GFAP-immunoreactive structures (green colour) (Fig. 8J) were usually found surrounding the SP (red colour) (Fig. 8K,L), but generally GFAP and Aß structures did not show coexistence (Fig. 8L). Occasionally, GFAP structures contained granular deposits of Aß reaction product. The GFAP structures showed a stellate morphology and numerous short processes, which were distributed in intimate relation to the external wall of blood vessels.

Electron microscopy

The immunohistochemical analysis was performed on sections from the postmortem brains of AD patients corresponding to CDR 3 scale. The Aß expression was found in large-neuron cell bodies with badly preserved cytoplasmic structure related to postmortem artifacts and edema. The rounded nucleus displayed several small, electrondense chromatin aggregates (Fig. 9A,B).

Aß immunoreactive deposits, as granular masses or filamentous accumulations of different sizes and morphology, were distributed throughout the perikaryon. These immunoreactive masses surrounded or were included in the mitochondria (Fig. 9E), the Nissl bodies, the granular ER (Fig. 9C,D), or were freely distributed

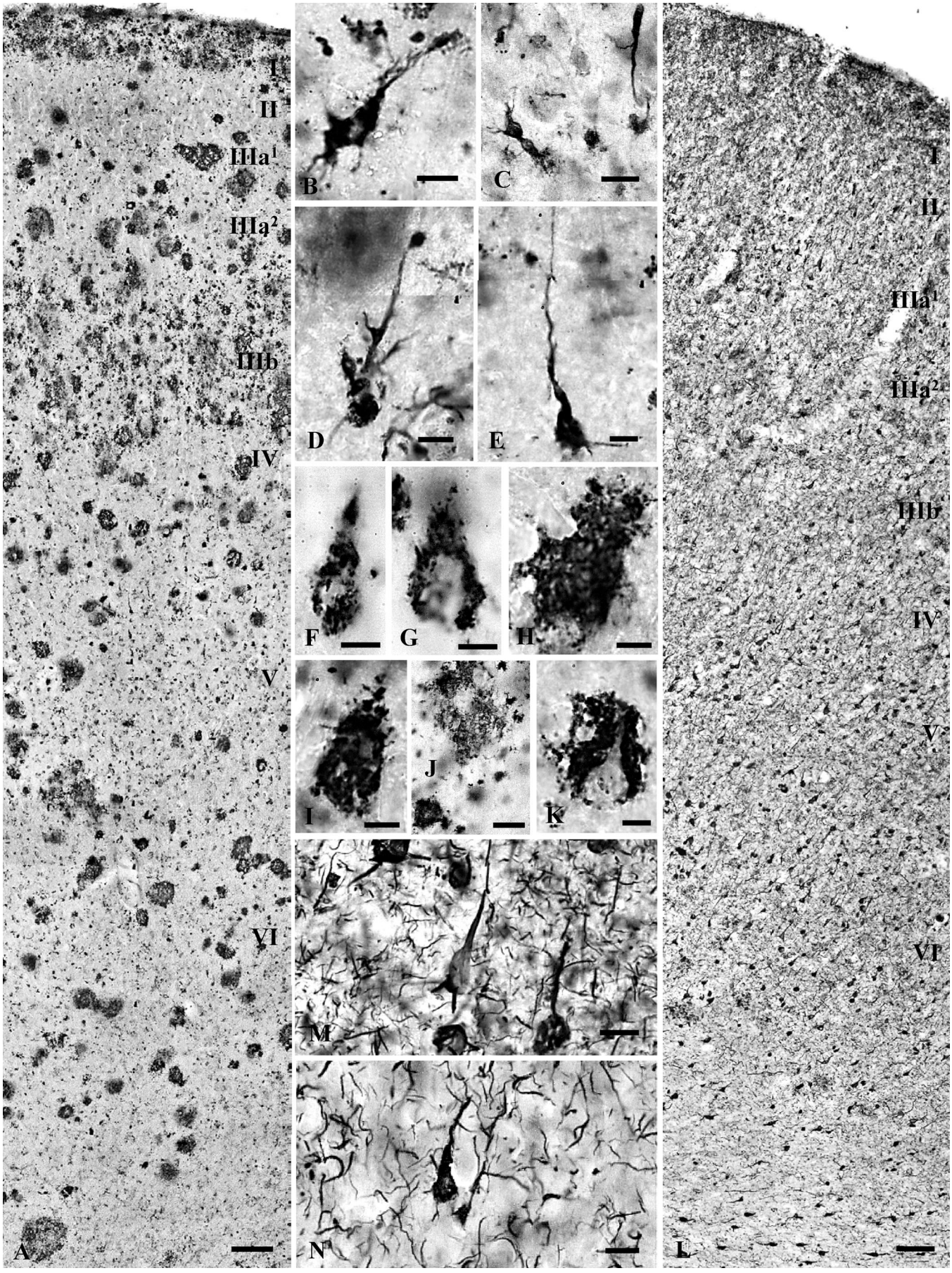

Fig. 7. Aß **(A)** and PHF **(L)** expression and distribution in the cerebral temporal cortex from postmortem brains of AD patients, CDR3. **B-G.** Morphological Aß structures in small pyramidal-like neurons (**B**, layer III; **D, E**, both layer V), glial cells **(C)** in layer V, and large pyramidal-like neurons in layer IIIb **(F, G, I)**. **H, J and K** show morphologically different senile plaques containing unreactive neurons in layers II, IIIb, and V, respectively. **M and N.** PHF immunoreactive neurons and dystrophic neurites in layers IIIb and V. Scale bars: A,L, 100 μm; B-E, J, K, M, N, 20 μm; F-I, K, 10 μm.

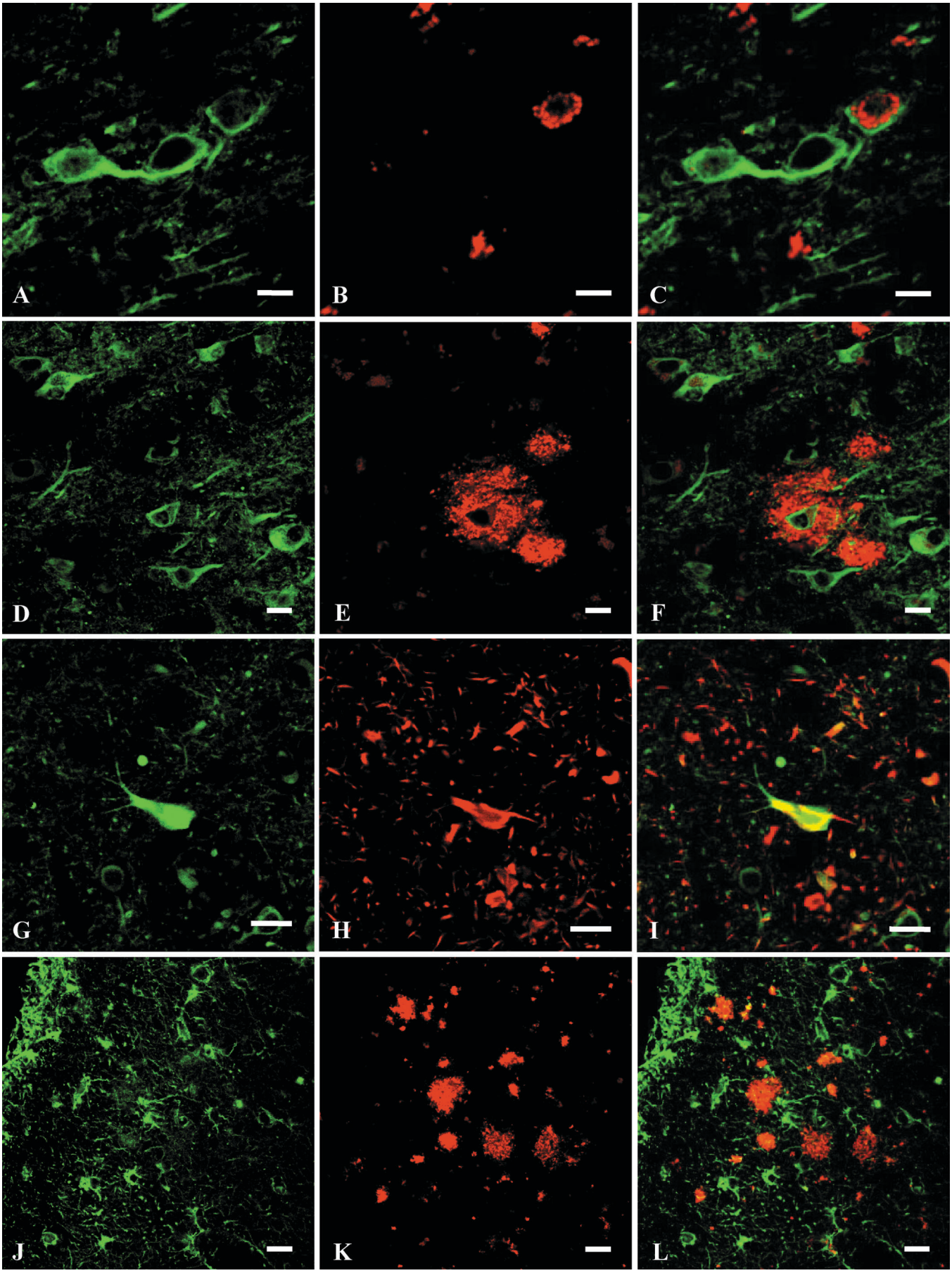

Fig. 8. Confocal microscope microphotographs to demonstrate the coexistence and colocalization between PGP/Aß **(A-F)**, PGP/PHF **(G-I)**, and GFAP/Aß **(J-L)** in CDR 3 scale. Some PGP-immunoreactive neurons (green colour) contain intracytoplasmic Aß (**C**, red colour). Aß reaction product (red colour) surrounds or includes PGP-immunoreactive neurons (green colour) **(F)**. Some PGP-immunoreactive neurons contain intracytoplasmic PHF reactivity **(I)**. Glial cells (green colour) are associated to masses of Aß of different size (red colour) **(L).** Scale bars: 20 μm.

through the perikaryon. Special distribution of this reaction product was found surrounding or included in the bodies of lipofuscin (Fig. 9F, G).

Quantification of Aß and PHF

The number of senile plaques was increased throughout the CDR scale with respect to the control group, reaching the highest levels in CDR 3 (Table 1). On the contrary, a progressive increase in the number of neurons containing Aß was found from the control group to the CDR 2 group, decreasing dramatically in CDR3. The number of Aß-immunoreactive glial cells increased from CDR 0.5 to CDR 3 with respect to control and preclinical individuals. The number of neuritic plaques visualized by PHF immunoreactivity was increased

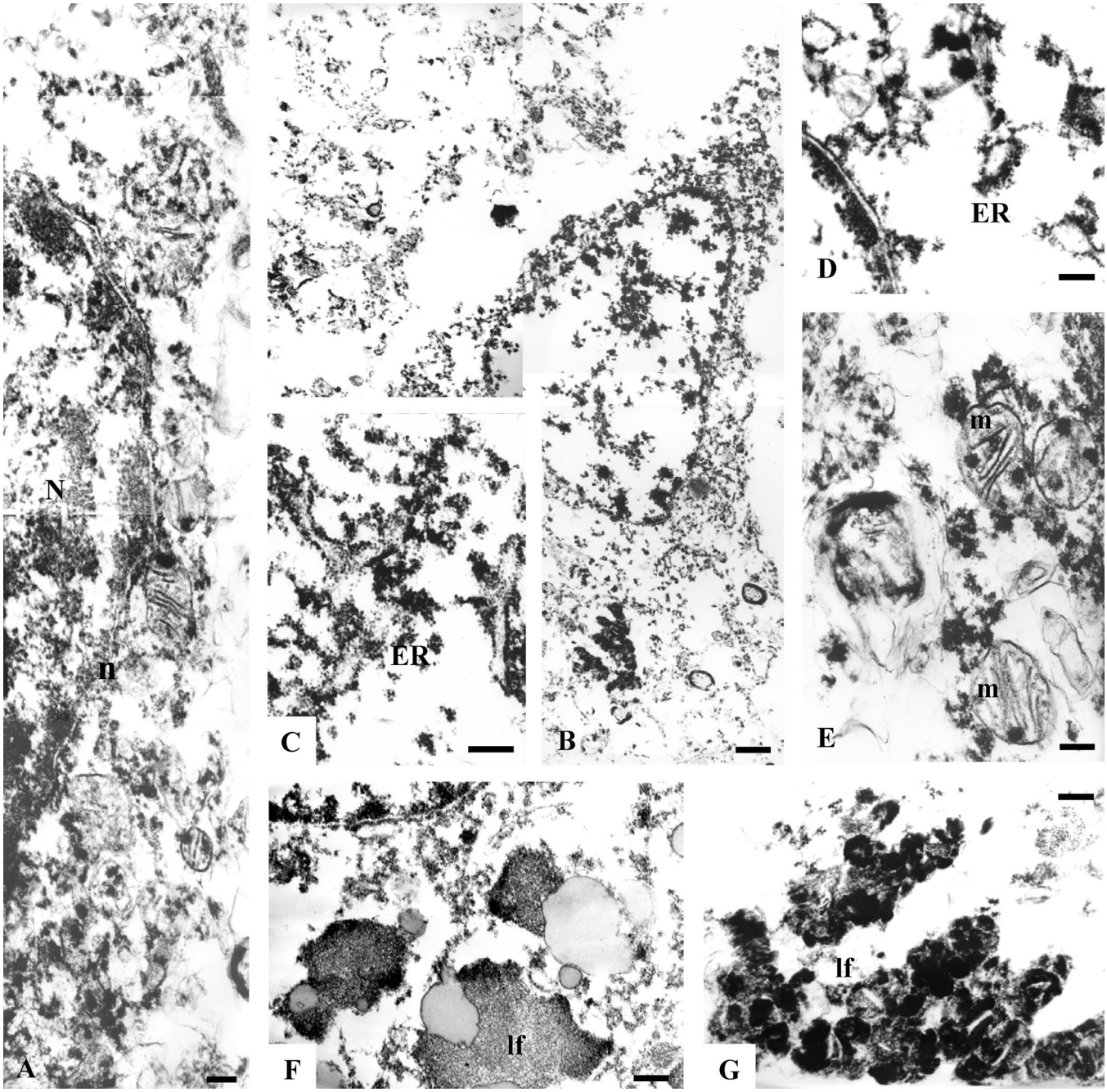

Fig. 9. Electron microphotographs from the temporal cortex, CDR 3, showing intracellular Aß deposits freely distributed in the perikaryon **(A, B)**, in relation to the granular endoplasmic reticulum **(C, D)**, in the external mitochondrial membrane **(E)** and in lipofuscin granules **(F, G)**. m: mitochondria; ER: endoplasmic reticulum; n: nuclear membrane; N: nucleus; lf: lipofuscin granule. Scale bars: A, C, D, E, G, 200 nm; B, 1 μm; F, 500 nm.

throughout the CDR scale with respect to the control group. The PHF-immunoreactive neurons progressively increased throughout the CDR scale, being dramatically increased in CDR3 (Table 1).

Discussion

Our results are focused on the demonstration of the chronic expression of Aß peptide and PHF

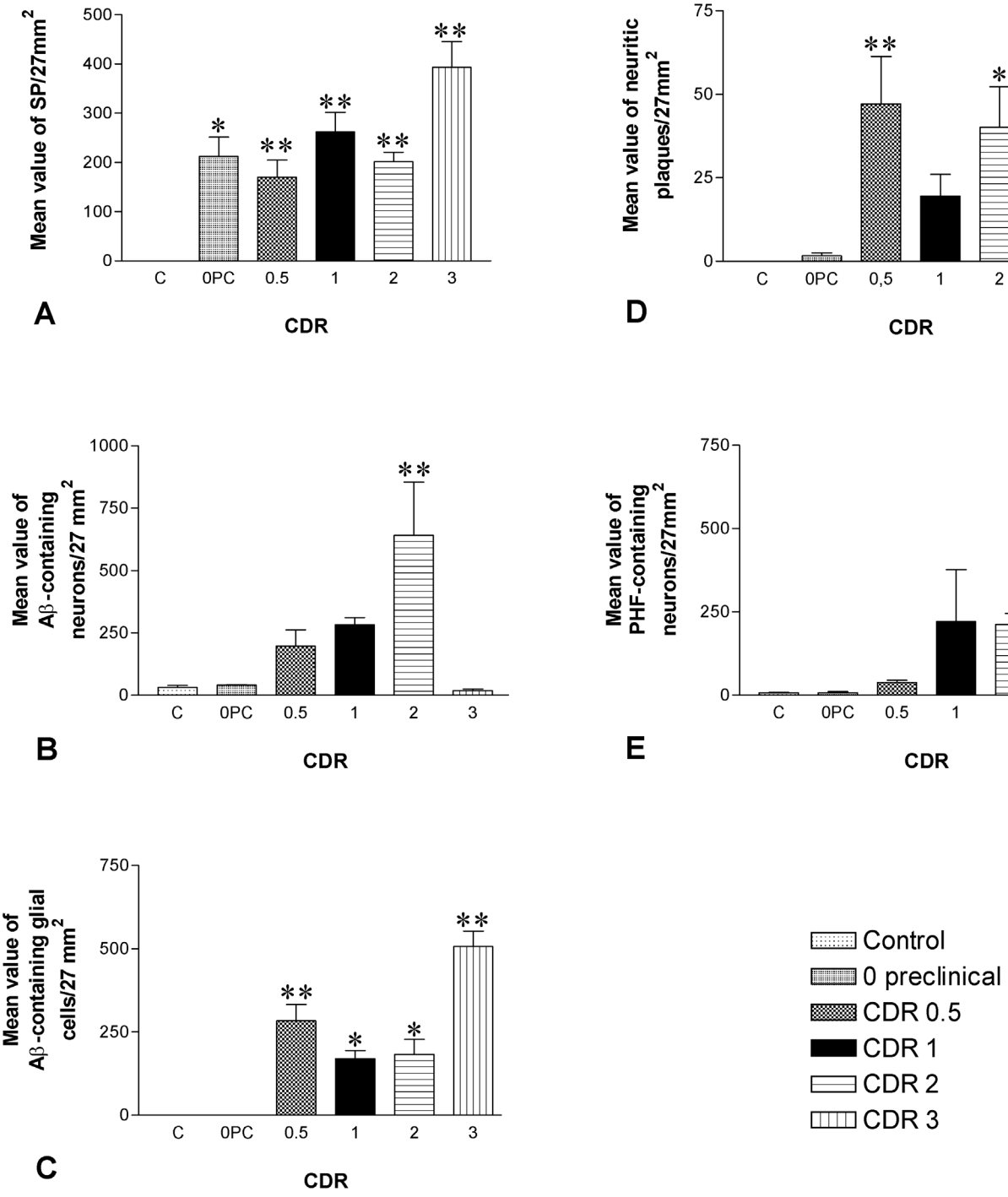

Table 1. Graphs showing variations in number of senile plaques (**A**), neurons with intracellular Aß (**B**), Aß immunoreactive glial cells (**C**), neuritic plaques (**D**), and PHF-immunoreactive neurons (**E**) in areas of 27 mm^2 of the temporal cortex from postmortem brains of AD patients ranging from CDR 0 to CDR 3. * $p<0.05$, ** $p<0.01$ versus control as analyzed by one-way ANOVA and afterwards the Dunnet test.

morphologically and immunohistochemically, as the main neuropathological markers of AD, in the cerebral temporal cortex from clinically evaluated individuals. The presence or absence of dementia was clinically assessed in all cases studied and the severity of the dementia clinically rated in all AD patients, according to the neuropathologically validated Clinical Dementia Rating (CDR) scale (Berg, 1988; Burke et al., 1988; Morris et al., 1988, 1991; Price et al., 1991; Morris, 1997; Price and Morris, 1999). The senile dementia of AD type was the only mental disorder found to be present as assessed by validated criteria (Berg et al., 1982; Morris, 1993, 1997). We have demonstrated by light immunohistochemistry the complete and progressive presence of numerous Aß-containing pyramidal neurons and SP in all AD stages studied. Intraneuronal Aß deposition has been confirmed by double immunohistochemistry with PGP 9.5 and Aß antibodies and its subcellular distribution addressed by electron microscopy. We have made the first description of two Aß-containing structures that displayed a pyramidal morphology with a reaction product that curiously resembles the appearance of that in senile plaques. One of these Aß-containing structures displayed the morphology of a pyramidal neuron not only with the soma stained, but also with the proximal portions of the apical and basal dendrites. These could be interpreted as various stages of a process of intracellular Aß deposition, neuronal death, and plaque formation. These findings demonstrate that SP might be produced as intracellular Aß deposits in neurons. It is possible that SP formation is mainly related to a lysis mechanism (D'Andrea et al., 2001). This changes could explain the disruption of the neuronal cytoskeleton, loss of synapses, neurons, and cortico-cortical connectivity found in AD (Jellinger, 1998), contributing to global alterations in multiple neurotransmitter systems, by means of pyramidal neuron dysfunction and posterior death.

Intracellular Aß deposition in pyramidal cortical neurons could be explained by intracellular production of Aß. It is has been demostrated that both Aß40 and Aß42 can be produced intracellularly (Wertkin et al., 1993) and furthermore, although much of the intracellularly generated Aß is on route to secretion, there is a significant pool of Aß that is not secreted (Cook et al., 1997; Wild-Bode et al., 1997; Skovronsky et al., 1998) and remains within the cell.

Recently, taking into account that neuronal cell death is a prominent feature of AD (Cotman and Su, 1996), it was proposed (Wilson et al., 1999) that the dying neurons might rupture and release the accumulated intracellular Aß42 into the surrounding extracellular parenchyma, and that once released Aß42 could have multiple effects. First, Aß42 might stimulate further production of amyloidogenic APP fragments in neighbouring neurons. Second, it might stimulate the releasing of the insoluble intracellular Aß42 from dying neurons and form a nidus for the accumulation of secreted Aß into diffuse or mature extracellular deposition of Aß plaques, as was previously found (LaFerla et al., 1997). The neuritic plaques, which may be detected by some specific molecular markers like tau (Dickson et al., 1988; Yan et al., 1994), normally colocalize with a dense neuronal sprouting (Ramón y Cajal, 1928) or atrophic projections (Mann et al., 1985) and also contains several cell types such as neurons, astrocytes, and microglia, which might be stimulated by and contribute to plaque formation (Geddes et al., 1986; Ihara, 1988; Cotman et al., 1991; Pike et al., 1995; Malchiodi-Albedi et al., 2001).

According to this, ultrastructurally, we have demonstrated deposits of Aß protein in cortical neurons that showed pyramidal-like morphology. These were distributed throughout the perikaryon, associated to the mitochondria, the Nissl bodies, the granular ER or freely distributed through the perikaryon in neurons with a badly preserved cytoplasmic structure. As has been previously stated (Wilson et al., 1999), the ER, the Golgi apparatus, and the endosomal/lysosomal systems might participate in the production of Ab deposits. The endosomal/lysosomal system contains APP (Selkoe, 1997) following reinternalization from the cell surface of the amyloidogenic APP carboxy-terminal, whose fragments have been demonstrated to exist in the endosomes/lysosomes, where they may serve as a substrate for γ-secretion cleavage to generate Aß (Koo and Squazzo, 1994). The Aß produced in this organelle is rapidly secreted (Tienari et al., 1997), contributing to a small amount of the Aß secreted pool to form extracellular Aß deposits (Wilson et al., 1999).

N2a cells that overexpress APP with the Swedish mutation tend to produce APP via ß-secretase cleavage to form Aß (Thinakaran et al., 1996; Xu et al., 1997). The intracellular localization of this ß-cleavage was investigated by blocking the APP in the ER with a fungal antibiotic. This abolished secreted Aß (Martin et al., 1995) as well as intracellular Aß40, demonstrating that these species were produced downstream of the ER. The specific location in the Golgi apparatus was determined by treatment of N2a cells with the ionophore monensin or incubation at 20°C, both of which block proteins trafficking in the trans-Golgi network, revealing that the Golgi apparatus is the main site of intracellular Aß42 (Xu et al., 1997). This Golgi processing also appears to be constitutively active in neurons expressing wild-type APP (Forman et al., 1997). Furthermore, this evidence about the source in neurons was also demonstrated by electron microscopy using an Aß40 end-specific antibody, which recognized the Aß40 in the trans-Golgi network (Hartmann et al., 1997; Greenfield et al., 1999).

The ER/intermediate components are the third pathway for the production of Aß (Cook et al., 1997; Hartmann et al., 1997; Wild-Bode et al., 1997). Immunoelectron microscopy studies confirm that Aß42 can be localized to the ER in neurons (Hartmann et al., 1997; Greenfield et al., 1999), so this Aß42 is not destined for secretion (Cook et al., 1997; Hartmann et

al., 1997; Wild-Bode et al., 1997).

In parallel, a progressive appearance of a variable number of neurodegenerative lesions containing PHF (i.e. NFT, distrophic neurites in neuritic plaques, and neuropil threads) were found in the temporal cortex as a vulnerable brain region.

There is a correlation between the severity of dementia (CDR 0-CDR 3) and the progressive increase in neurons containing intracellular Aß deposits, SP, neuritic plaques, neuropil threads, and NFT, the layer I being the last layer to show Aß- and PHF-immunoreactive structures. On the contrary, layers III and V were the most readily affected by intracellular Aß deposition, which is consistent with the fact that layers III and V are vulnerable subpopulations of the temporal cortex in AD. In addition, we have also found that the deposition of the Aß peptide is a neuropathological finding prior to the appearance of PHF-immunoreactive structures in the temporal cortex.

Aß was detected intracellularly within neuronal cells such as NT2N (Wertkin et al., 1993; Turner et al., 1996; Skovronsky et al., 1998; Wilson et al., 1999), in microglia cell types (Kuentzel et al., 1993; Fuller et al., 1995; Morelli et al., 1999), in primary neuronal cultures derived from cerebral cortex of embryonic day-15 (E15) CD1 mice (Gouras et al., 2000), and in a subpopulation of neurons of AD patients (Mochizuki et al., 2000; Bayer et al., 2001). Immunohistochemical analyses have recently revealed that intracellular Aß staining preceded plaque deposition (Wirths et al., 2001). However, it has recently been postulated that Aß may have an intracellular origin prior to secretion (Cras et al., 1990; Wilson et al., 1999, Takahashi et al., 2002).

We have also provided the first evidence of the presence of Aß peptide deposition in cortical pyramidal neurons of non-demented individuals. Only occasional SP were found in only one individual in this CDR 0 scale. The successive CDR scales increased in number of Aß-immunoreactive neurons and SP.

This work provides evidence for an intracellular origin of senile plaques in humans as a substrate for the synaptic and neuronal loss and cortico-cortical disconnection characteristic of the AD.

Acknowledgements. This study was supported by a Grant from the Fundación La Caixa 99/077-40. We thank Dr. Joseph Price and the clinicians and staff of the Alzheimer Center at Washington University in St. Louis (Supported by grants P01 AG03991 and P50 AG05681 from the US National Institute on Aging) for supplying brain sections from clinically and pathologically assesed aging and Alzheimer's Disease cases. We thank also D. Nesbitt for his help in the manuscript preparation.

References

Arendt T. (1993). Neuronal dedifferentiation and degeneration in Alzheimer's disease. Biol. Chem. Hopp-Seyler 374, 911-912.

Arendt T. (2000). Alzheimer's disease as a loss of differentiation control in a subset of neurons that retain immature features in the adult brain. Neurobiol. Aging 21, 783-796.

Arendt T., Zvegintseva H.G. and Leontovich T.A. (1986). Dendritic changes in the basal nucleus of Meynert and in the diagonal band nucleus in Alzheimer's disease-a quantitative golgi investigation. Neuroscience 198, 1265-1278.

Arendt T., Schindler C., Bruckner M.K., Eschrich K., Bigl V., Zedlick D. and Marcova L. (1997). Plastic neuronal remodelling is impaired in patients with Alzheimer's disease carrying apolipoprotein e4 allele. J. Neurosci. 17, 516-529.

Arendt T., Brückner M.K., Gertz H.J. and Marcova L. (1998). Cortical distribution of neurofibrillary tangles in Alzheimer's disease matches the pattern of neurones that retain their capacity of plastic remodelling in the adult brain. Neuroscience 83, 991-1002.

Arriagada P.V., Growden J.H., Hedley-Whyte E.T. and Hyman B.T. (1992). Neurofibrillary tangles but not senile plaques parallel duration and severity of Alzheimer's disease. Neurology 42, 631-639.

Augustinack J.C., Schneider A., Mandelkow E.M. and Hyman B.T. (2002). Specific tau phosphorylation sites correlate with severity of neuronal cytopathology in Alzheimer's disease. Acta Neuropathol. (Berl) 103, 26-35.

Bacskai B.J., Kajdasz S.T., Christie R.H., Carter C., Garmes D., Seubert P., Schenk D. and Hyman B.T. (2001). Imaging of amyloid-beta deposits in brains of living mice permits direct observation of clearance of plaques with immunotherapy. Nat. Med. 7, 369-372.

Bacskai B.J., Kajdasz S.T., McLellan M.E., Games D., Seubert P. and Hyman B.T. (2002). Non-Fc-mediated mechanisms are involved in clearance of amyloid-beta in vivo by immunotherapy. J. Neurosci. 22, 7873-7878.

Ball M.J. (1977). Neuronal loss, neurofibrillary tangles and granulovacuolar degeneration in the hippocampus with aging and dementia. A quantitative study. Acta Neuropathol. 37, 111-118.

Ball M.J. (1978). Topographic distribution of neurofibrillary tangles and granulovascular degeneration in hippocampal cortex of aging and demented patients: a quantitative study. Acta Neuropathol. 42, 73-80.

Balldin J., Gottfries C.G., Karlsson G., Lindstedt G., Langstrom G. and Walinder J. (1983). Dexamethasone suppression test and serum prolactin in dementia disorders. Br. J. Psychiat. 143, 277-281.

Bayer T.A., Wirths O., Majtényi K., Hartmann T., Multhaup G., Beyreuther K. and Czech C. (2001). Key factors in Alzheimer's disease: ß-amyloid precursor protein processing, metabolism and intraneuronal transport. Brain Pathol. 11, 1-11.

Berg L. (1988). Clinical dementia rating (CDR). Psychopharmacol. Bull. 25, 637-639.

Berg L., Hughes C.P., Coben L.A., Danziger W.L., Martin R.L. and Knesevich J. (1982). Mild senile dementia of Alzheimer type: Research diagnostic criteria, recruitment, and description of a study population. J. Neurol. Neurosurg. Psychiat. 45, 962-968.

Berg L., McKeel D.W., Miller Jr J.P., Baty J. and Morris J.C. (1993). Neuropathological indexes of Alzheimer's disease in demented and nondemented persons aged 80 years and older. Arch. Neurol. 50, 349-358.

Blessed G., Tomlinson B.E. and Roth M. (1968). The association between quantitative measures of dementia and of senile change in the cerebral grey matter of elderly subjects. Br. J. Psychiat. 114, 797-811.

Bondareff W., Wischik C.M., Novak M., Amos W.B., Klug A. and Roth

M. (1990). Molecular analysis of neurofibrillary degeneration in Alzheimer's disease. An immunohistochemical study. Am. J. Pathol. 137, 711-723.

Braak H. and Braak E. (1991). Neuropathological staging of Alzheimer-related changes. Acta Neuropathol. 82, 239-259.

Braak H. and Braak E. (1992). The human entorhinal region. Normal morphology and lamina-specific pathology in various diseases. Neurosci. Res. 15, 6-31.

Braak E., Braak H. and Mandelkow E.M. (1994). A sequence of cytoskeleton changes related to the formation of neurofibrillary tangles and neuropil threads. Acta Neuropathol. 87, 554-567.

Burke W.J., Miller J.P., Rubin E.H., Morris J.C., Coben L.A., Duchek J., Wittels I.G. and Berg L. (1988). Reliability of the Washington University Clinical Dementia Rating. Arch. Neurol. 45, 31-32.

Byne W., Mattiace L., Kress Y. and Davies P. (1991). Alz-50 immunoreactivity in the hypothalamus of the normal and Alzheimer human and the rat. J. Comp. Neurol. 306, 602-612.

Caputo C.B., Wischik C., Novak M., Scott C.W., Brunner W.F., Montejo de Garcini E., Lo M.M.S., Norris T.E. and Salama A.I. (1992). Immunological characterization of the region of tau protein that is bound to Alzheimer paired helical filaments. Neurobiol. Aging 13, 267-274.

Christie J.E., Whalley L.J., Bennie J., Dick H., Blackburn M., Blackwood D.H. and Fink G. (1987). Characteristic plasma hormone changes in Alzheimer's disease. Br. J. Psychiat. 150, 674-681.

Cook D.G., Forman M.S., Sung J.C., Leight S., Kolson D.L., Iwatsubo T., Lee W.M. and Doms R.W. (1997). Alzheimer's Aß(1-42) is generated in the endoplasmic reticulum/intermediate compartment of NT2N cells. Nat. Med. 3, 1021-1023.

Cotman C.W. and Su J.H. (1996). Mechanism of neuronal death in Alzheimer's disease. Brain Pathol. 6, 493-506.

Cotman C.W., Cummings B.J. and Whitson J.S. (1991). The role of misdirected plasticity in plaque biogenesis and Alzheimer's disease pathology. In: Growth factors and Alzheimer's disease. Heft F., Brachet P., Wil B. and Christen Y. (eds.). Springer-Verlag. Berlin. pp 222-233.

Cras P., Kawai M., Siedlak S., Mulvihill P., Gambetti P., Lowery D., Gonzalez-DeWhitt P., Greenberg B. and Perry G. (1990). Neuronal and microglial involvement in ß-amyloid protein deposition in Alzheimer's disease. Am. J. Pathol. 137, 241-246.

Crystal H., Dickson D., Fuld P., Masur D., Scott R., Mehler M., Masdeu J., Kawas C., Aronson M. and Wolfson L. (1988). Clinicopathological studies in dementia: nondemented subjects with pathologically confirmed Alzheimer's disease. Neurology 38, 1682-1687.

D'Andrea M.R.D., Nagale R.G., Wang H.Y., Peterson P.A. and Lee D.H. (2001). Evidence that neurons accumulating amyloid can undergo lysis to form amyloid plaques in Alzheimer's disease. Histopathology 38, 120-134.

Davies L., Wolska B., Hilbich C., Multhaup G., Martins R., Simms G., Beyreuther K. and Masters C.L. (1988). A4 amyloid protein deposition and the diagnosis of Alzheimer's disease: Prevalence in aged brains determined by immunocytochemistry compared with conventional neuropathologic techniques. Neurology 38, 1688-1693.

DeKosky S.T. and Scheff S.W. (1990). Synapse loss in frontal cortex biopsies in Alzheimer's disease: Correlation with cognitive severity. Ann. Neurol. 27, 457-464.

Delaere P., Duyckaerts C., Masters C., Beyreuther K., Piette F. and Hauwn J.J. (1990). Large amounts of neocortical beta/A4 deposits without neuritic plaques nor tangles in a psychometrically assessed, non-demented person. Neurosci. Lett. 116, 87-93.

Dickson D.W., Farlo J., Davies P., Crystal H., Fuld P. and Yen S.C., (1988). Alzheimer's disease. A double-labelling immunohistochemical study of senile plaques. Am. J. Pathol. 132, 86-101.

Dickson D.W., Crystal H.A., Mattiace L.A., Masur D.M., Blau A.D., Davies P., Yen S-H. and Aronson M.K. (1991). Identification of normal and pathological aging in prospectively studied nondemented elderly humans. Neurobiol. Aging 13, 179-189.

Forman M.S., Cook D.G., Leight S., Doms R.W. and Lee V.M.-Y. (1997). Differential effects of the Swedish mutant amyloid precursor protein on ß-amyloid accumulation and secretion in neurons and non-neuronal cells. J. Biol. Chem. 272, 32247-32253.

Frenkel D., Balass M. and Solomon B. (1998). N-terminal EFRH sequence of Alzheimer's beta-amyloid peptide represents the epitope of its anti-aggregating antibodies. J. Neuroimmunol. 88, 85-90.

Frenkel D., Balass M., Katchalski-Katzir E. and Solomon B. (1999). High affinity binding of monoclonal antibodies to the sequential epitope EFRH of beta-amyloid peptide is essential for modulation of fibrillar aggregation. J. Neuroimmunol. 95, 136-142.

Fuller S.J., Storey E., Li X.Q., Smith A.I., Beyreuther K. and Masters C.I. (1995). Intracellular production of ßA4 amyloid of Alzheimer's disease: modulation by phosphoramidon and lack of coupling to the secretion of the amyloid precursor protein. Biochemistry 34, 8091-8098.

Gandy S. and Greengard P. (1992). Amyloidogenesis in Alzheimer's disease: some possible therapeutic opportunities. Trends. Pharmacol. Sci. 13, 108-113.

Geddes J.W., Anderson K.J. and Cotman C.W. (1986). Senile plaques as aberrant sprout-stimulating structures. Exp. Neurol. 94, 767-776.

German D.C., White C.L. and Sparkman D.R. (1987). Alzheimer's disease: Neurofibrillary tangles in nuclei that project to the cerebral cortex. Neuroscience 21, 305-312.

Gomez-Isla T., Growdon W.B., McNamara M.J., Nochlin D., Bird T.D., Arango J.C., Lopera F., Kosic K.S., Lantos P.L., Caims N.J. and Hyman B.T. (1999). The impact of different presenilin 1 and presenilin 2 mutations on amyloid deposition, neurofibrillary changes and neuronal loss in the familial Alzheimer's disease brain: evidence for other phenotype-modifying factors. Brain 122, 1709-1719.

Good P.F., Werner P., Hsu A., Olanow C.W. and Perl D.P. (1996). Evidence for neuronal oxidative damage in Alzheimer's disease. Am. J. Pathol. 143, 21-28.

Gouras G.K., Tsai J., Naslund J., Vincent B., Edgar M., Checler F., Greenfield J.P., Haroutunian V., Buxbaum J.D., Xu H., Greengard P. and Relkin N.R. (2000). Intraneuronal Aß42 accumulation in human brain. Am. J. Pathol. 156, 15-20.

Grammas P. (2000). A damaged microcirculation contributes to neuronal cell death in Alzheimer's disease. Neurobiol. Aging 21, 199-205.

Greenberg S.G., Davies P., Schein J.D. and Rinder L.I. (1992). Hidrofluoric acid-treated tPHF proteins display the same biochemical properties as normal t**.** J. Biol. Chem. 267, 564-569.

Greenfield J.P., Tsai J., Gouras G.K., Hai B., Thinakaran G., Checler F., Sisodia S.S., Greengard P. and Xu H. (1999). Endoplasmic reticulum and trans-Golgi network generate distinct populations of Alzheimer ß-amyloid peptides. Proc. Natl. Acad. Sci. USA 96, 742-747.

Guesdon J.L., Ternyck T. and Avrameas S. (1981). The use of avidin-biotin interaction in immunoenzymatic techniques. J. Histochem.

Cytochem. 27, 1131-1139.

Gyure K.A., Durham R., Stewart W.F., Smialek J.E. and Troncoso J.C. (2001). Intraneuronal abeta-amyloid precedes development of amyloid plaques in Down syndrome. Arch. Pathol. Lab. Med. 125, 489-492.

Hartmann T., Bieger S.C., Brühl B., Tienary P.J., Ida N., Allsop D., Roberts G.W., Masters C.L., Dotti C.G., Unsicker K. and Beyreuther K. (1997). Distinct sites of intracellular production for Alzheimer's disease AB40/42 amyloid peptides. Nat. Med. 3, 1016-1020.

Hasegawa M., Jakes R., Goether R.A., Lee V.M.-Y., Ihara Y. and Goedert M. (1996). Characterization of mAb AP422, a novel phosphorylate-dependent monoclonal antibody against tau protein. FEBS Lett. 384, 23-30.

Heintz N. (1993). Cell-death and the cell-cycle-a relationship between transformation and neurodegeneration. Trends. Biochem. Sci. 18, 157-159.

Hirano A. and Zimmerman H.M. (1962). Alzheimer's neurofibrillary changes: A topographic study. Arch. Neurol. 7, 227-242.

Hoffmann R., Lee V.M.-Y., Leight S., Varga I., and Otvos Jr. L. (1997). Unique Alzheimer's disease paried helical filaments specific epitopes involve double phosphorilation at specific sites. Biochemistry 36, 8114-8124.

Hsu S.M. and Raine L. (1981). Protein A, avidin, and biotin in immunohistochemistry. J. Histochem. Cytochem. 29, 1349-1353.

Hyman B.T., Van Hoesen G.W., Damasio A.R. and Barnes C.L. (1984). Alzheimer's disease: cell specific pathology isolates the hippocampal formation. Science 225, 1168-1170.

Hyman B.T., Van Hoesen G.W., Wolozin B.L., Davies P., Kromer L.J. and Damasio A.R. (1988). Alz-50 antibody recognizes Alzheimer-related neuronal changes. Ann. Neurol. 23, 371-379.

Hyman B.T., Tanzi R.E., Marzloff K., Barbour R. and Schenk D. (1992). Kunitz protease inhibitor-containing amyloid, protein precursor immunoreactivity in Alzheimer's disease. J. Neuropathol. Exper. Neurol. 51, 76-83.

Iacono R.P. and Sandyck R. (1987). Alzheimer's disease and the pivotal role of the hypothalamus and the intrinsic opioid syste. Int. J. Neurosci. 32, 711-714.

Ihara Y. (1988). Massive somatodendritic sprouting of cortical neurons in Alzheimer's disease. Brain Res. 459, 138-144.

Ishii T. (1966). Distribution of Alzheimer's neurofibrillary changes in the brain stem and hypothalamus of senile dementia. Acta Neuropathol. 6, 1-7.

Jellinger K.A. (1998). The neuropathological diagnosis of Alzheimer's disease. J. Neural Transm. Suppl. 53, 97-118.

Jellinger K.A. and Bancher C. (1998). Neuropathology of Alzheimer's disease: a critical update. J. Neural Transm. Suppl. 54, 77-95.

Katzman R., Terry R.D., DeTeresa R., Brown T., Davies P., Fuld P., Renbing X. and Peck A. (1988). Clinical, pathological, and neurochemical changes in dementia: a subgroup with preserved mental status and numerous neocortical plaques. Ann. Neurol. 23, 138-144.

Kondo J., Honda T., Mori H., Hamada Y., Miura R., Ogawara M. and Ihara Y. (1988). The carboxyl third of tau is tightly bound to paired helical filaments. Neuron 1, 827-834.

Koo E.H. and Squazzo S. (1994). Evidence that production and release of amyloid b-protein involves the endocytic pathway. J. Biol. Chem. 269, 17386-17389.

Kuentzel S.L., Ali S.M., Altman R.A., Greenberg B.D. and Raub T.J. (1993). The Alzheimer ß-amyloid protein precursor/protease nexin-II is cleaved by secretase in a trans-Golgi secretory compartment in human neuroglioma cells. J. Biochem. 295, 367-378.

LaFerla F.M., Troncoso J.C., Strickland D.K., Kawas C.H. and Jay G. (1997). Neuronal cell death in Alzheimer's disease correlates with apoE uptake and intracellular Abeta stabilization. J. Clin. Invest. 100, 310-320.

Lang E., Szendrei G.I., Lee V.M.-Y. and Otvos Jr L. (1992). Immunological and conformational characterization of a phosphorylated immunodominant epitope on the paried helical filaments found in Alzheimer disease. Biochem. Biophys. Res. Commun. 181, 783-790.

Liao A., Nitsch R.M., Greenberg S.M., Finckh U., Blacker D., Albert M., Rebeck G.W., Gomez-Isla T., Clabworthy A., Binetti G., Hock C., Mueller-Thormsen T., Mann U., Zuchowski K., Beisiegel U., Staehelin H., Growdon J.H., Tanzi R.E. and Hyman B.T. (1998). Genetic association of an alpha2-macroglobulin (Val1000Ile) polymorphism and Alzheimer's disease. Hum. Mol. Genet. 12, 1953-1956.

Malchiodi-Albedi F., Domenici M.R., Paradisi S., Bernardo A., AjmoneCat M.A. and Minghetti L. (2001). Astrocytes contribute to neuronal impairment in beta A toxicity increasing apoptosis in rat hippocampal neurons. Glia 34, 68-72.

Mann D.M.A. and Esiri M.M. (1989). The pattern of acquisition of plaques and tangles in the brains of patients under 50 years of age with Down's syndrome. J. Neurol. Sci. 89, 169-179.

Mann D.M., Yates P.O. and Marcyniuk B. (1985). Correlation between senile plaque and neurofibrillary tangle counts in cerebral cortex and neuronal counts in cortex and subcortical structures in Alzheimer's disease. Neurosci. Lett. 56, 51-55.

Martin B.L., Schrader-Fischer G., Busciglio J., Duke M., Paganetti P. and Yanker B.A. (1995). Intracellular accumulation of ß-amyloid in cells expressing the Swedish mutant amyloid precursor protein. J. Biol. Chem. 270, 26727-26730.

Masliah E., Terry R.D., DeTeresa R.M. and Hansen L.A. (1989). Immunohistochemical quantification of the synapse-related protein synaptophysin in Alzheimer disease. Neurosci. Lett. 103, 234-239.

McKee A.C., Kosik K.S. and Kowall N.W. (1991). Neuritic pathology and dementia in Alzheimer's disease. Ann. Neurol. 30, 156-165.

Mochizuki A., Tamaoka A., Shimohata A., Komatsuzaki Y. and Shoji S. (2000). Aß42-positive non-pyramidal neurons around amyloid plaques in Alzheimer's disease. Lancet 355, 42-43.

Morelli L., Prat M.I. and Castaño E.M. (1999). Differential accumulation of soluble amyloid b peptides 1-40 and 1-42 in human monocytic and neuroblastoma cell lines. Cell. Tissue Res. 298, 225-232.

Morris J.C. (1993). The clinical dementia rating (CDR): Current version and scoring rules. Neurology 43, 2412-2414.

Morris J.C. (1997). Clinical Dementia Rating: A reliable and valid diagnostic and staging measure for dementia of the Alzheimer type. Int. Psychogeriatr. Suppl. 9, 173-176.

Morris J.C., McKeel D.W., Fulling K., Torack R.M., and Berg L. (1988). Validation of clinical diagnostic criteria for Alzheimer's disease. Ann. Neurol. 24, 17-22.

Morris J.C., McKeel D.W., Storandt J.R., Rubin E.H., Price J.L., Grant E.A., Berg L. and Ball M.J. (1991). Very mild Alzheimer's disease: Informant-based clinical, psychometric and pathologic distinction from normal aging. Neurology 41, 469-78.

Morris J.C., Storandt M., McKeel D.W., Rubin E.H., Price J.L., Grant E.A. and Berg L. (1996). Cerebral amyloid deposition and diffuse plaques in "normal" aging: Evidence for presymptomatic and very

mild Alzheimer's disease. Neurology 46, 707-719.

Nagy Z., Esiri M.M., Cato A.M. and Smith A.D. (1997). Cell cycle markers in the hippocampus in Alzheimer's disease. Acta Neuropathol. 94, 6-15.

Novak M., Kabat J. and Wischik C.M. (1993). Molecular characterization of the minimal protease resistant tau-unit of the Alzheimer's disease paired helical filament. EMBO J. 12, 365-370.

Otvos L., Feiner L., Lang E., Szendrei G.I., Goedert M. and Lee V.M. (1994). Monoclonal antibody PHF-1 recognizes tau protein phosphorylated at serine residues 396 and 404. J. Neurosci. Res. 39, 669-673.

Parvizi J., Van Hoesen G.W. and Damasio A. (2000). Selective pathological changes of the periaqueductal gray matter in Alzheimer's disease. Ann. Neurol. 48, 344-353.

Parvizi J., Van Hoesen G.W. and Damasio A. (2001). The selective vulnerability of brainstem nuclei to Alzheimer's disease. Ann. Neurol. 49, 53-66.

Pike C.J., Cummings B.J. and Cotman C.W. (1995). Early association of reactive astrocytes with senile plaques in Alzheimer's disease. Exp. Neurol. 132, 172-179.

Price J.L. and Morris J.C. (1999). Tangles and plaques in nondemented aging and "preclinical" Alzheimer's disease. Ann. Neurol. 45, 358-368.

Price J.L., Davis P.B., Morris J.C. and White D.L. (1991). The distribution of tangles, plaques and related immunohistochemical markers in healthy aging and Alzheimer's disease. Neurobiol. Aging 12, 295-312.

Ramón y Cajal S. (1928). Degeneration and regeneration of the nervous system. Vol II. Hafner Publishing Company. London.

Raskind M., Peskind E., Rivard M.F., Veith R. and Barnes R. (1982). Dexamethasone suppression test and cortisol circadian rhythm in primary degenerative dementia. Am. J. Psychiat. 139, 1468-1471.

Rodrigo J., Springall D., Uttenthal O., Bentura M.L., Riveros V., Abadia-Molina F., Martínez-Murillo R., Polak J.M. and Moncada S. (1994). Localization of nitric oxide synthase in the adult rat brain. Phil. Trans. R. Soc. London B 345, 175-221.

Rothchild D. (1937). Pathologic changes in senile psychoses and their pathobiologic significance. Am. J. Psychiat. 93, 757-784.

Saper C.B. and German D.C. (1987). Hypothalamic pathology in Alzheimer's disease. Neurosci. Lett. 74, 364-370.

Schenk D. (2002). Amyloid-beta immunotherapy for Alzheimer's disease: the end of the beginning. Nat. Rev. Neurosci. 3, 824-828.

Selkoe D.J. (1994). Cell biology of the amyloid b-protein precursor and the mechanism of Alzheimer's disease. Annu. Rev. Cell Biol. 10, 373-403.

Selkoe D.J. (1997). Cellular and molecular biology of ß-amyloid precursor and Alzheimer's disease. In: The molecular and genetic basis of neurological disease. Prusiner S.B., Rosenberg R.N. and Mauro S.D. (eds). Butterworth Heinemann Press. Boston. pp 601-602.

Skovronsky D.M., Doms R.W. and Lee V.M. (1998). Detection of a novel intraneuronal pool of insoluble amyloid ß protein that accumulates with time in culture. J. Cell Biol. 14, 1031-1039.

Spar J.E. and Gerner R. (1982). Does the dexamethasone suppression test distinguish dementia from depression? Am. J. Psychiat. 139, 238-240.

Takahashi R.H., Nam E.E., Edgar M. and Gouras G.K. (2002). Alzheimer ß-amyloid peptides: normal and abnormal localization. Histol. Histopathol. 17, 239-246.

Terry R.D. (1994). Neuropathological changes in Alzheimer's disease. Prog. Brain. Res. 101, 383-390.

Terry R.D. and Katzman R. (1983). Senile dementia of the Alzheimer type: defining a disease. In: The neurology of aging. Katzman R. and Terry R.D. (eds.) Contemporary Neurology. Series Philadelphia Davis. Boston. pp 51-84.

Terry R.D., Hansen L.A., DeTeresa R., Davies P., Tobias H. and Katzman R. (1987). Senile dementia of the Alzheimer type without neocortical neurofibrillary tangles. J. Neuropathol. Exp. Neurol. 46, 262-268.

Terry R.D., Masliah E., Salmon D.P., Butters N., DeTeresa R., Hill R., Hansen L.A. and Katzman R. (1991). Physical basis of cognitive alterations in Alzheimer's disease: Synapse loss is the major correlate of cognitive impairment. Ann. Neurol. 30, 572-580.

Thinakaran G., Borchelt D.R., Lee M.K., Slunt H.H., Spitzer L., Kim G., Ratovitsky T., Davenport F., Nordstedt C., Seeger M., Hardy J., Levey A.I., Gandy S.E., Jenkins N.A., Copeland N.G., Price D.L. and Sisodia S.S. (1996). Endoproteolysis of presenilin-1 and accumulation of processed derivatives in vivo. Neuron 17, 181-190.

Tienari P.J., Ida N., Ikonen E., Simons M., Weidemann A., Multhaup G., Masters C.L., Dotti C.G. and Beyreuthe K. (1997). Intracellular and secreted Alzheimer ß-amyloid species are generated by distinct mechanisms in cultured hippocampal neurons. Proc. Natl. Acad. Sci. USA 94, 4125-4130.

Tomlinson B.E., Blessed G. and Roth M. (1968). Observations on the brains of nondemented old people. J. Neurol. Sci. 7, 331-356.

Tucker H.M., Kihiko-Ehmann M., Wright S., Rydel R.E. and Estus S. (2000). Tissue plasminogen activator requires plasminogen to modulate amyloid-beta neurotoxicity and deposition. J. Neurochem. 75, 2172-2177.

Turner R.S., Suzuki N., Chyung A.S.C., Younkin S.G. and Lee V.M.-Y. (1996). Amyloids ß40 and ß42 are generated intracellularly in human neurons and their secretion increases with maturation. J. Biol. Chem. 27, 8966-8970.

Ulrich J. and Stahelin H.B. (1984). The variable topography of Alzheimer's type changes in senile dementia and normal old age. Gerontology 30, 210-214.

Ulrich J., Anderton B.H., Brion J.P., Euler M. and Probst A. (1987). Cytoskeletal immunohistochemisty of Alzheimer's disease. J. Neural. Transm. Suppl. 24, 197-204.

Urbanc B., Cruz L., Buldyrev S.V., Havlin S., Irizarry M.C., Stanley H.E. and Hyman B.T. (1999). Dynamics of plaque formation in Alzheimer's disease. J. Biophys. 76, 1330-1334.

Uttenthal L.O., Alonso D., Fernández A.P., Campbell R.O., Moro M.A., Leza J.C., Esteban F.J., Barroso J.B., Valderrama R., Pedrosa J.A., Peinado M.A., Serrano J., Richart A., Bentura M.L., Santacana M., Martínez-Murillo R., Rodrigo J. (1998). Neuronal and inducible nitric oxide synthase and nitrotyrosine immunoreactivities in the cerebral cortex of the aging rat. Microsc Res Techniq 43, 75-88.

Walker L.C., Price D.L., Voytko M.L. and Schenk D.B. (1994). Labelling of cerebral amyloid in vivo with a monoclonal antibody. J. Neuropathol. Exp. Neurol. 53, 377-383.

Wertkin A.M., Turner R.S., Pleasure S.J., Golde T.E., Younkin S.G., Trojanowski J.Q. and Lee V.M.-Y. (1993). Human neurons derived from a teratocarcinoma cell line express solely the 695-amino acid amyloid precursor protein and produce intracellular b-amyloid or A4 peptides. Proc. Natl. Acad. Sci. USA 90, 9513-9517.

Wild-Bode C., Yamazaki T., Capell A., Leimer U., Steiner H., Ihara Y. and Haass C. (1997). Intracellular generation and accumulation of

amyloid b-peptide terminating at amino acid 42. J. Biol. Chem. 272, 16085-16088.

Wilson C.A., Doms R.W. and Lee V.M.-Y. (1999). Intracellular APP processing and Ab production in Alzheimer disease. J. Neuropathol. Exp. Neurol. 58, 787-794.

Wirths O., Multhaup G., Czech C., Blanchard V., Moussaoui S., Tremp G., Pradier L., Beyreuther K. and Bayer T.A. (2001). Intraneuronal A, accumulation precedes plaque formation in ß-amyloid precursor protein and presenilin-1 double-transgenic mice. Neurosci. Lett. 306, 116-120.

Wischik C.M., Novak M., Thogersen H., Edwards P., Runswick M., Jakes R., Walker J., Milstein C., Roth M. and Klug A. (1988). Isolation of a fragment of tau derived from the core of the paired helical filament of Alzheimer disease. Proc. Natl. Acad. Sci. USA 85, 4506-4510.

Xu H., Sweeney D., Wang R., Thinakaran G., Lo A.C., Sisodia S.S., Greengard P. and Gandy S. (1997). Generation of Alzheimer b-amyloid protein in the trans-Golgi network in the apparent absence of vesicle formation. Proc. Natl. Acad. Sci. USA 94, 3748-3752.

Yan S.D., Chen X., Schmidt A.M., Brett J., Godman G., Zou Y.S., Scott C.W., Caputo C., Frappier T., Smith M.A., Perry G., Yen S.H., Stern D. (1994). Glycated tau protein in Alzheimer disease: A mechanism for induction of oxidant stress. Proc. Natl. Acad. Sci. USA 91, 7787-7791.

Accepted March 25, 2004